Investigation of the impact damage due to high-energy objects on the wreckage of flight MH17

Customer

Dutch Safety Board

NLR-CR-2015-155-PT-1 - September 2015

Source cover picture: ANP

National Aerospace Laboratory NLR
Anthony Fokkerweg 2
1059 CM Amsterdam
The Netherlands
Tel +31 (0)88 511 3113
www.nlr.nl

EXECUTIVE SUMMARY

Investigation of the impact damage due to high-energy objects on the wreckage of flight MH17

Problem area

The Dutch National Aerospace Laboratory (NLR) was asked by the Dutch Safety Board (DSB) to participate in the investigation of the impact damage due to high-energy objects on the wreckage of flight MH17. This investigation was performed by the Defence Systems Department of the NLR.

Description of work

The impact damage due to high-energy objects on the wreckage of flight MH17 was investigated. To investigate the possible cause of this damage, three scenarios using different classes of weapon systems in use in the region were analysed.

Results and conclusions

Damage examination

Based upon the damage examination it is concluded that the impact damage on the wreckage of flight MH17 is caused by a warhead with various types of preformed fragments in the 6-14 mm size range, including one type with a bowtie shape, detonating to the left of, and above, the cockpit.

Scenario 1: Air-to-Air Gun

The damage observed on the wreckage is not consistent with the damage caused by an air-to-air gun in number of hits, density of hits, direction of trajectories and type of damage. The high-energy object damage on the wreckage of flight MH17 is therefore not caused by an air-to-air gun.

Report no.
NLR-CR-2015-155-PT-1

Author(s)
J. Markerink

Report classification
UNCLASSIFIED

Date
September 2015

Knowledge area(s)
Safety & Security
Weapon Systems

Descriptor(s)
MH17
crash
investigation
Malaysia Airlines
Boeing 777

Scenario 2: Air-to-Air Missile

The damage observed on the wreckage is not consistent with the damage caused by the warhead of an air-to-air missile in use in the region in amount of damage, type of damage and type of fragments. The high-energy object damage on the wreckage of flight MH17 is therefore not caused by an air-to-air missile.

Scenario 3: Surface-to-Air Missile

Of the investigated warheads only the 9N314M contains the unique bowtie shaped fragments found in the wreckage. The damage observed on the wreckage in amount of damage, type of damage, boundary and impact angles of damage, number and density of hits, size of penetrations and bowtie fragments found in the wreckage, is consistent with the damage caused by the 9N314M warhead used in the 9M38 and 9M38M1 BUK surface-to-air missile.

Conclusion

Based on the results of the investigation it is concluded that the high-energy object damage observed on the wreckage of flight MH17 is caused by the 9N314M warhead used in the 9M38 and 9M38M1 BUK surface-to-air missile.

Investigation of the impact damage due to high-energy objects on the wreckage of flight MH17

J. Markerink

Customer
Dutch Safety Board

September 2015

Customer	Dutch Safety Board
Owner	Dutch Safety Board
Division NLR	Air Transport
Distribution	Unlimited
Classification of title	Unclassified
Date	September 2015

Content

Abbreviations

Acronym	Description
CAS	Close Air Support
CP	Command Post
DSB	Dutch Safety Board
FDR	Flight Data Recorder
NATO	North Atlantic Treaty Organization
NLR	National Aerospace Laboratory NLR
SAM	Surface-to-Air Missile
TAR	Target Acquisition Radar
TAS	True Airspeed
TELAR	Transporter Erector Launcher and Radar
TELL	Transporter Erector Launcher and Loader
WEST	Weapon Engagement Simulation Tool
WVR	Within Visual Range

This page is intentionally left blank.

1 Introduction

The Dutch Safety Board (DSB) investigates the crash of the Boeing 777-200, Malaysia Airlines flight MH17, on 17 July 2014 in the east of Ukraine. The purpose of this investigation is to establish the causes of the crash and in particular, the cause of the damage to the forward fuselage of the aircraft. In the preliminary report the Dutch Safety Board states that the damage to the forward part of the fuselage appears to indicate that there were impacts from a large number of high-energy objects from outside the aircraft [2.].

The Dutch National Aerospace Laboratory (NLR) was asked by the Dutch Safety Board to participate in the investigation of the impact damage due to high-energy objects on the wreckage of flight MH17. This investigation was performed by the Defence Systems Department of the NLR. This department provides operational, technical and scientific support to the Dutch Ministry of Defence in general, and the Royal Netherlands Air Force in particular. The main research subject is airborne self-protection, which requires an extensive knowledge of the performance of surface-to-air and air-to-air weapon systems. For this purpose the department has several tools at its disposal. One of these is WEST (Weapon Engagement Simulation Tool); an in-house developed software tool to simulate the flyout and performance of threat systems. A number of WEST models are used in this investigation.

The work was performed as follows: First, the damage on the wreckage was thoroughly examined and quantified. Once the physical evidence was investigated, the known characteristics of all relevant air-to-air guns, air-to-air missiles, and surface-to-air missiles were systematically evaluated for possible consistency with the damage observed on the wreckage. Of the evaluated weapon systems, only one was found to be consistent with the observed damage. For this weapon system the detonation location, orientation and weapon trajectory were analysed in further detail.

The structure of this report is as follows: Chapter 2 provides details of the aircraft damage examination. The three scenarios, using different classes of weapon systems in use in the region, are specified in Chapter 3. Chapters 4 through 6 elaborate on the analysis of each scenario, discussing in particular consistency with the observed damage. Chapter 7 provides a summary of the findings and conclusions.

2 Damage examination

At the time the investigation commenced, around 25% of the wreckage was available to the Dutch Safety Board at Gilze-Rijen Air Force Base in The Netherlands (Figure 1 and Figure 2). The parts of interest to the investigation were located in one hangar. The remaining parts were located in two separate aircraft shelters. Of each part of the wreckage photographs were taken and these were made available for the investigation. Also a number of 3D laser scans of parts of the wreckage were made and used in this investigation.

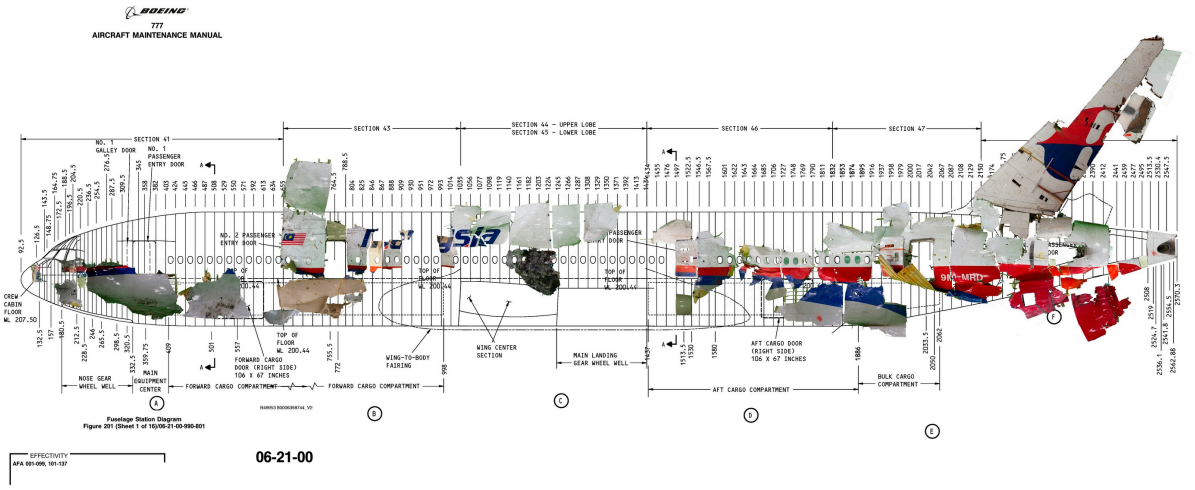

Figure 1: Left-hand side recovered wreckage (Source: DSB)

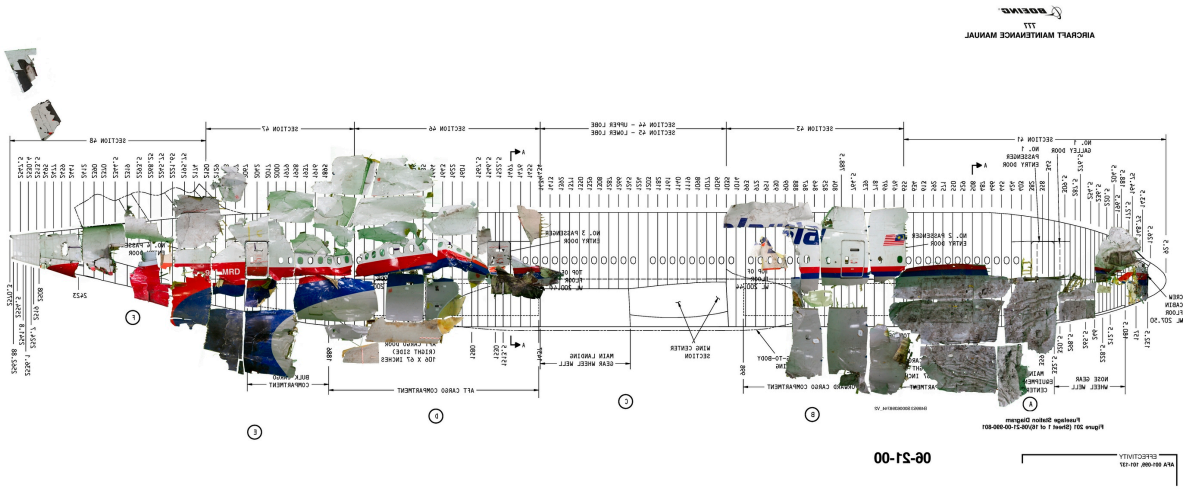

Figure 2: Right-hand side recovered wreckage (Source: DSB)

2.1 Types of observed impact damage

The impact damage due to the high-energy objects was investigated on the wreckage of the cockpit.

Four types of impact damage [1] were identified:

1. Piercing damage. In piercing damage the high-energy object penetrates the plate by pushing the plate material aside. The high-energy object tears through the plate during penetration, and a crown-shaped protrusion surrounded by radial cracks is formed on the exit side of the plate.
2. Plugging damage. In plugging damage the high-energy object impacting the plate produces a relatively clean hole by shearing out a portion of the plate known as a plug.
3. Non-penetrating damage. Where relatively strong, thick and reinforced parts of the airframe structure were present; a number of high-energy objects did not have enough energy to fully penetrate the structure and produced non-penetrating damage.
4. Ricochet damage. When the angle of impact on a plate is shallow, the object will not be able to fully penetrate the structure and ricochets of the plate leaving non-penetrating ricochet damage.

Figure 3 through Figure 6 show examples of the different types of damage on the wreckage of flight MH17.

The impact damage found on the wreckage indicates that the aircraft was hit by a large number of high-energy objects of various shapes and sizes.

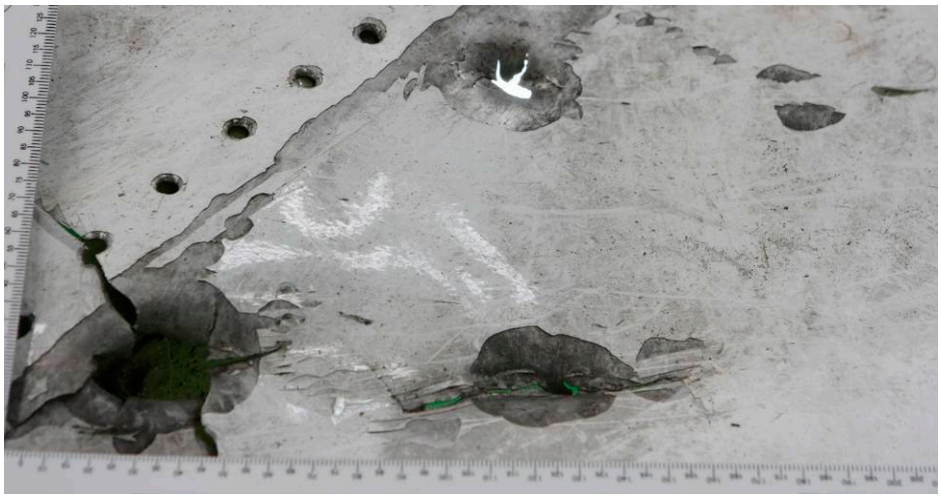

Figure 3: Piercing damage (Source: DSB)

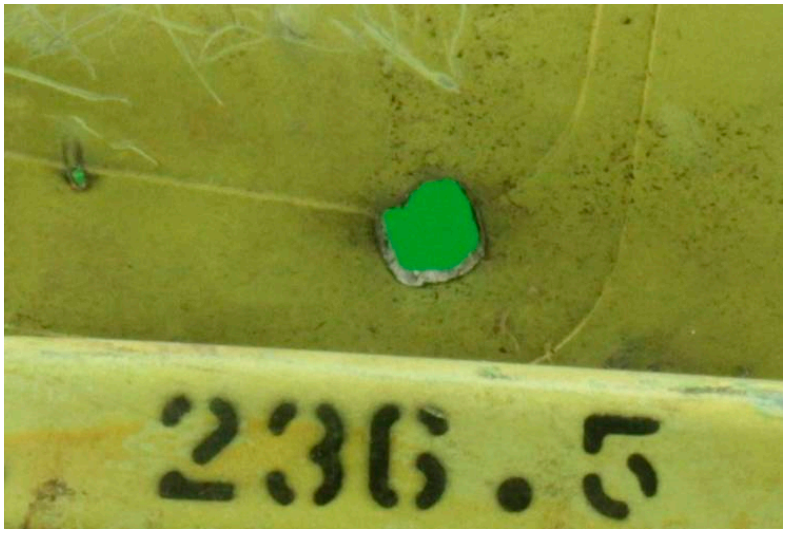

Figure 4: Plugging damage (Source: DSB)

Figure 5: Non-penetrating damage

Figure 6: Ricochet damage (Source: DSB)

2.2 Pitting

Besides the direct impact damage of high-energy objects found on the aircraft, pitting was also observed on some parts of the wreckage of the cockpit [3]. Pitting is a phenomenon that occurs on metal surfaces that are in proximity to detonating explosives and indicates the occurrence of an explosive event nearby (Figure 7).

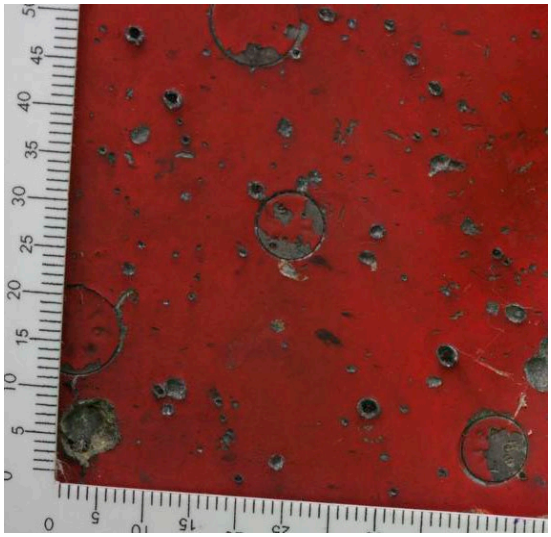

Figure 7: Pitting (Source: DSB)

2.3 Origin

The observed impact damage by high-energy objects originates from outside the aircraft. Both piercing and plugging damage observed are identified as entry damage bending the plate material inwards (Figure 8). The non-penetrating damage as well as the ricochet damage also clearly originates from outside the aircraft.

Figure 8: Plate material bent inwards. Looking at the inside of the structure

At certain parts of the structure, where multiple layers of plate material are riveted together, some high-energy objects impacted the structure at a shallow angle, penetrating the first outer plate but ricocheting back from the second plate and exiting through the outer plate. This creates the outer layer penetration damage as seen in Figure 9.

Figure 9: Outer layer penetration

2.4 Exit Damage

Exit damage is observed on the wreckage of the lower right-hand side of the cockpit (Figure 10). This is an indication of a direction of impact from the upper left-hand side of the cockpit towards the lower right-hand side of the cockpit.

Figure 10: Exit damage on lower right-hand side of the cockpit

2.5 Number and density of hits

The total number of hits of all types of impact damage on the initially available wreckage was counted and found to be 304. After this, additional parts of the wreckage became available. Accounting for the additional hits on these parts the total number of impacts is assessed to be more than 350. Extrapolating the number of hits on the affected area of the fuselage and accounting for the structure that was not available gives an estimate of the total number of hits of high-energy objects of over 800. The highest density of hits was on the middle window on the captain's left-hand side of the cockpit (window number 2). The cockpit windows are made of multiple layers of glass and plastic and one of the layers of this window was recovered. See Figure 11 for this window layer and its location in the cockpit. The density in this area is calculated to be around 250 hits per square meter.

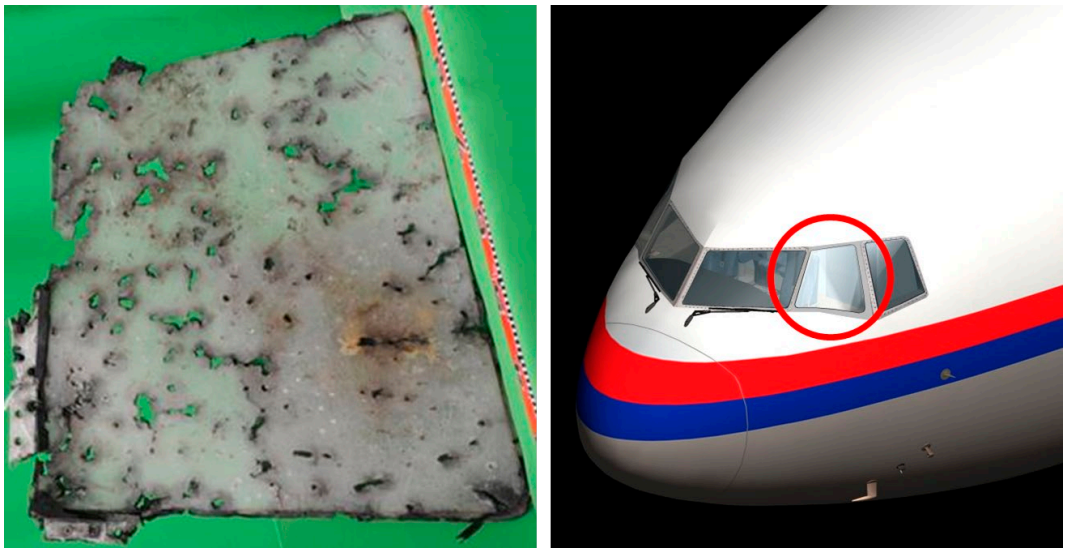

Figure 11: Left cockpit window 2 layer and location (Source: DSB)

2.6 Size of penetration damage

On the piece of cockpit skin with the highest number of penetrations, the size of the holes caused by these penetrations was measured (Figure 12). Only the damage that was assessed to be the result of single objects fully penetrating the plate was taken into account. Of each hole the dimension perpendicular to the impact direction was measured (Figure 13). Only this dimension gives an indication of the size of the object that caused the damage. The larger dimension, parallel to the projection of the impact direction on the plate, is the result of the speed and the angle at which the object impacts the plate. As can be seen in Figure 14, the size was found to range from 6 mm to 14 mm.

Figure 12: Piece of wreckage used for size of penetration measurement

Figure 13: Measurement of penetration damage

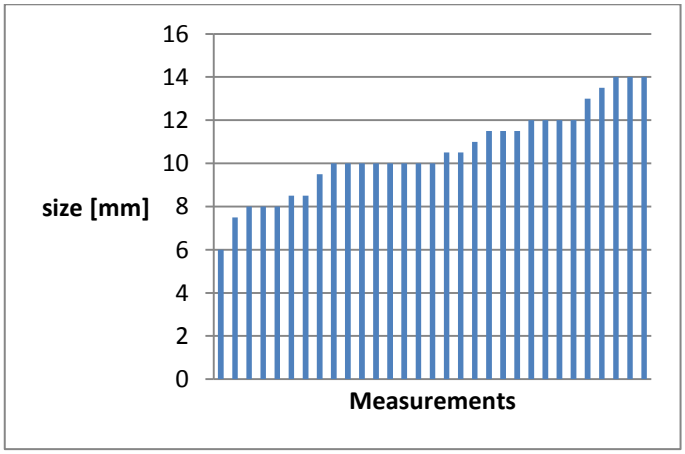

Figure 14: Size of penetration damage

2.7 Regularity of hits

On several parts of the wreckage a regularity of hits was observed. Figure 15 and Figure 16 are examples of hits at regular intervals. This regularity of hits is an indication that the damage was caused by a warhead with preformed, separate fragments. See section 6.10 for a more in depth discussion of this subject.

Figure 15: Regularity of hits on upper cockpit window frame

Figure 16: Regularity of hits on lower cockpit window frame

2.8 Location of damage

The main location of the impact damage of high-energy objects is on the left-hand and upper side of the cockpit. The right-hand side of the cockpit shows no high-energy object impact damage. In particular the two co-pilot's windows on the right-hand side show no penetration damage as can be seen in Figure 17.

Figure 17: Right-hand side of cockpit

2.9 Boundary of damage

There is a relatively clear boundary between parts of the wreckage that are affected by the high-energy object impacts and parts that are unaffected. On the front side of the cockpit, the boundary is the forward corner of the captain's (left-hand side) front window. Figure 18 shows this corner, together with the two windscreen wipers. The most forward impact damage occurs just above and aft (to the rear) of this corner as can be seen by the penetration damage in the glass.

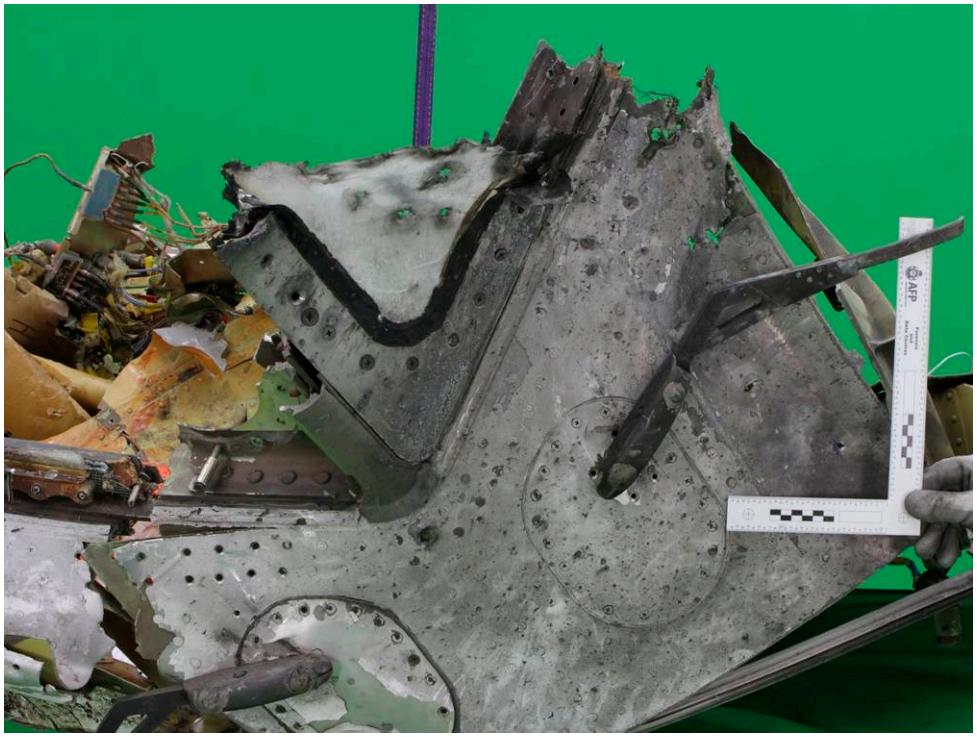

Figure 18: Forward corner of left-hand side cockpit front window (Source: DSB)

On the top and right-hand side of the cockpit the damage boundary is indicated by the ricochet impacts on the cockpit roof as shown in Figure 19. To the right (starboard side) of this area no impact damage is present.

Figure 19: Right-hand side cockpit roof (looking nose to tail)

The rearmost impact damage boundary is found on the left-hand side in front of the left-hand forward passenger door. Figure 20 through Figure 22 show the most rearward high-energy object ricochets.

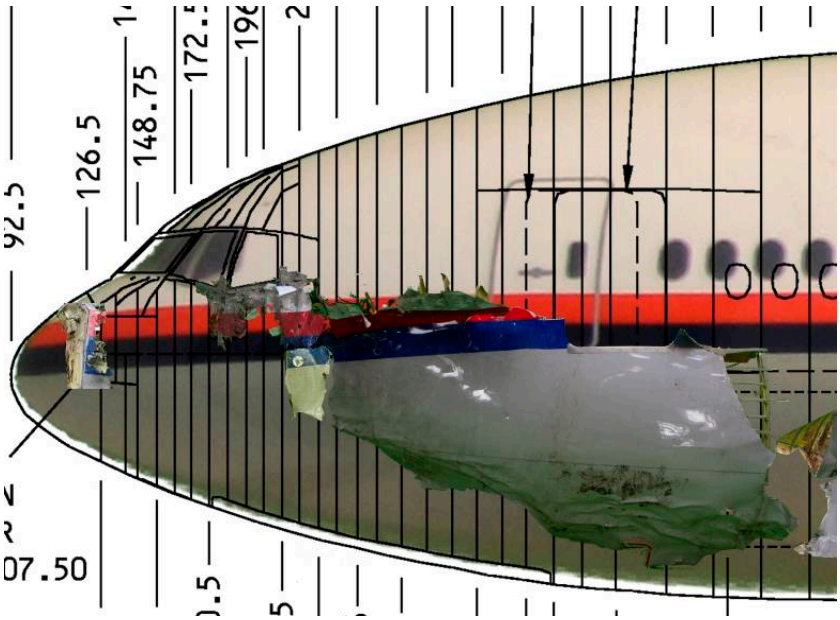

Figure 20: Left-hand side panel location (Source: DSB)

Figure 21: Left-hand side panel with ricochet damage

Figure 22: Detail of left-hand side panel ricochet damage

2.10 Direction of impact

To determine the high-energy objects trajectory, the direction of the impact damage was analysed on several parts of the cockpit area. Using fibreglass rods and 3D-scans of the structure, the direction of high-energy objects penetrating multiple layers of material was determined. The results of this analysis can be found in Figure 23 and Figure 24. Also the forensic technique of stringing was used to analyse the general direction of the impact damage on the actual wreckage as can be seen in Figure 25. The back traced trajectories of the penetrating damage converge to a general area to the left of, and above, the cockpit.

Figure 23: High-energy objects impact direction

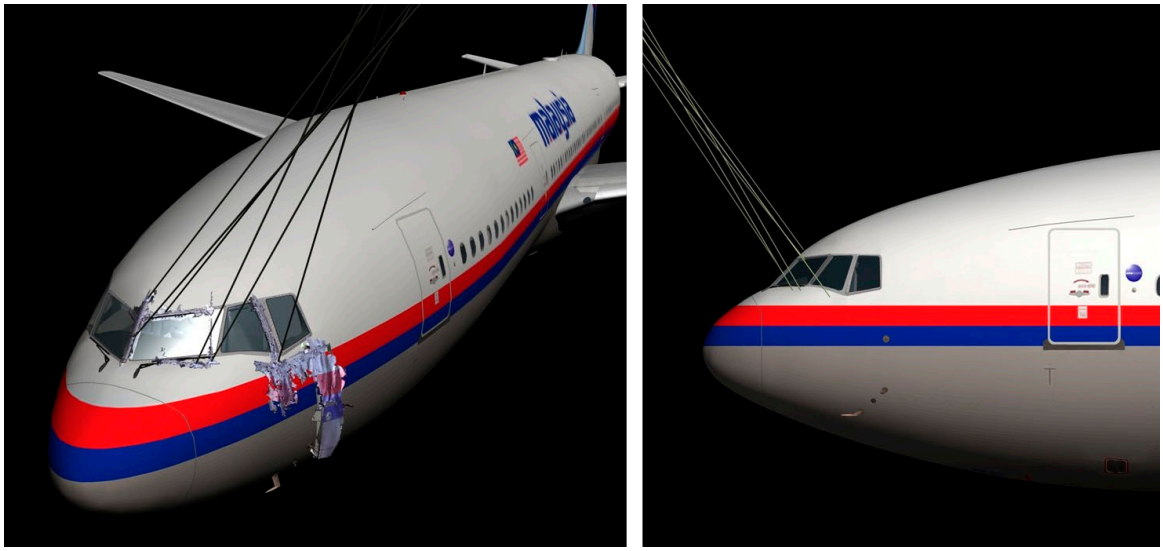

Figure 24: High-energy objects impact direction origin in 3D-scan

Figure 25: Stringing of high-energy objects impacts to determine general location of origin (Source: DSB)

For the non-penetrating ricochet and grazing hits the angle relative to the structure was measured to give a direction in the plane of the aircraft skin. This was done for the cockpit roof (Figure 26) and the left-hand side of the cockpit.

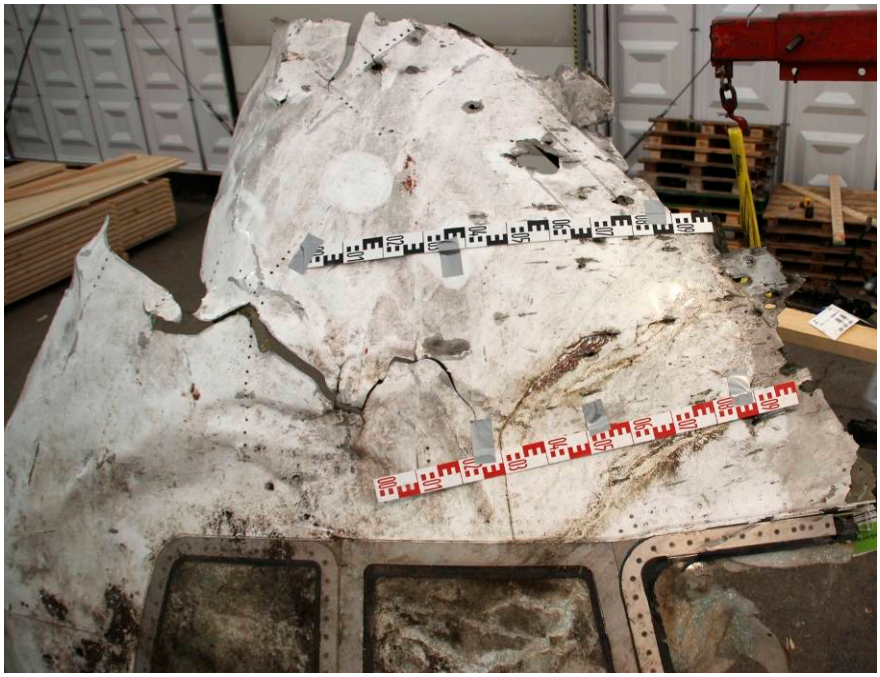

Figure 26: Rulers showing local direction of ricochet damage on cockpit roof

Because a piece of cockpit roof was not yet available to the Dutch Safety Board at the time of writing, the angle of ricochet damage on this piece was determined using photographs. This piece was located on the top of the cockpit, more to the rear of the aircraft. Figure 27 shows a detail of this cockpit roof. The flight direction is indicated with a blue arrow and the ricochet damage direction with a red arrow.

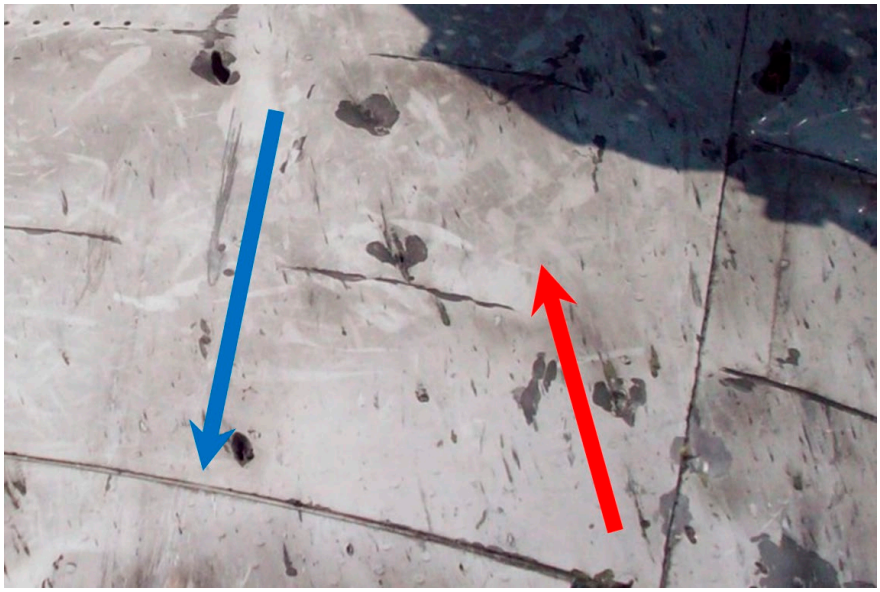

Figure 27: Direction of ricochet damage (red) on cockpit roof. Blue arrow indicates flight direction (Source: DSB)

Based on the analysis of the direction of both the penetrating and the non-penetrating high-energy object damage, all objects appear to originate from a general area to the left of, and above, the cockpit.

2.11 Other impact damage

Besides the main high-energy object impact damage on the cockpit there are two further areas where impact damage is observed: the left engine cowling ring and the left wingtip. The left engine cowling ring is a hollow structure consisting of an aerodynamically shaped curved front and a flat plate rear. A number of objects have penetrated both parts of this structure from the front to the rear and from this a trajectory direction can be derived. In Figure 28 and Figure 29 the front and rear plate penetrations caused by the same object has been indicated. In Figure 29 it is possible to look through both holes to obtain the direction of the line of sight through these holes. The engine cowling ring has been placed at the correct location with respect to the cockpit, of which the back side of the front bulkhead is visible on the right side of Figure 29. The observed penetrations show a general object trajectory direction originating from an area to the left of, and above, the cockpit. The size of the damage caused by objects that penetrated both front and rear plate is significantly larger than the impact damage found on the wreckage of the cockpit. The size of all penetrations of the front of the ring was measured and found to range from 1 to 200 mm. Only 5 of the 47 penetrations were in the same 6-14 mm size range as the ones found on the cockpit panel of Figure 14. None of the objects that caused these 5 penetrations also penetrated the back plate.

Figure 28: Impact damage on front side engine cowling ring

Figure 29: Impact damage on rear side engine cowling ring

On the left-hand wingtip upper surface, damage is observed from the front to the rear. The direction to the damage origin is in the general direction to an area slightly to the left of the cockpit, (Figure 30). All damage directions lead to the same general area as indicated in Figure 31.

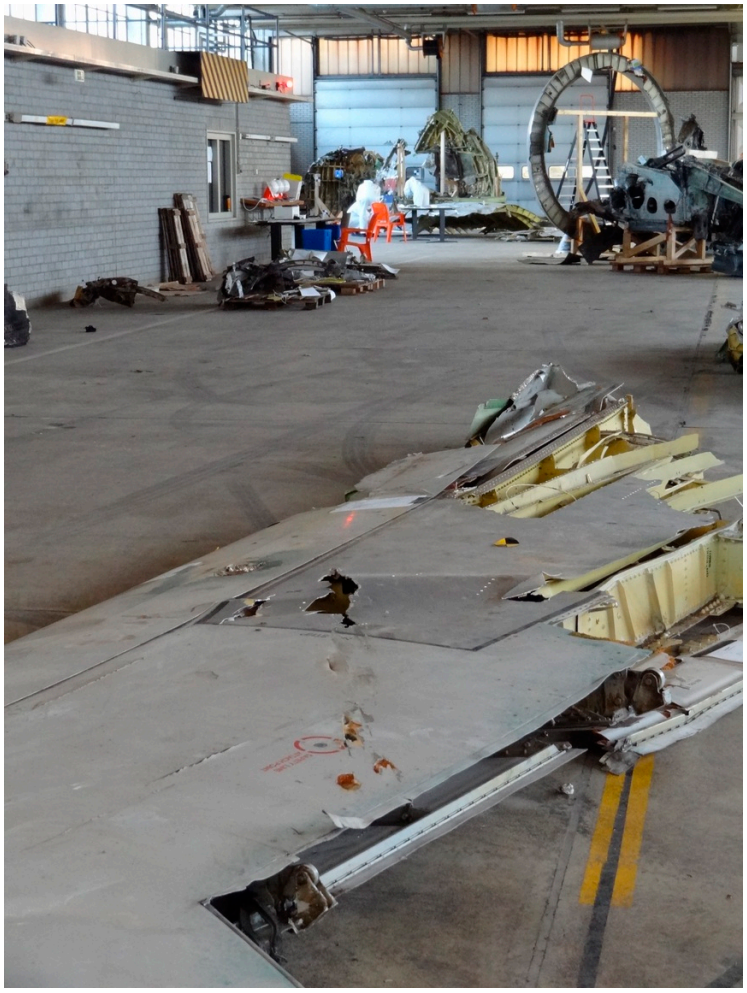

Figure 30: Damage to left wingtip

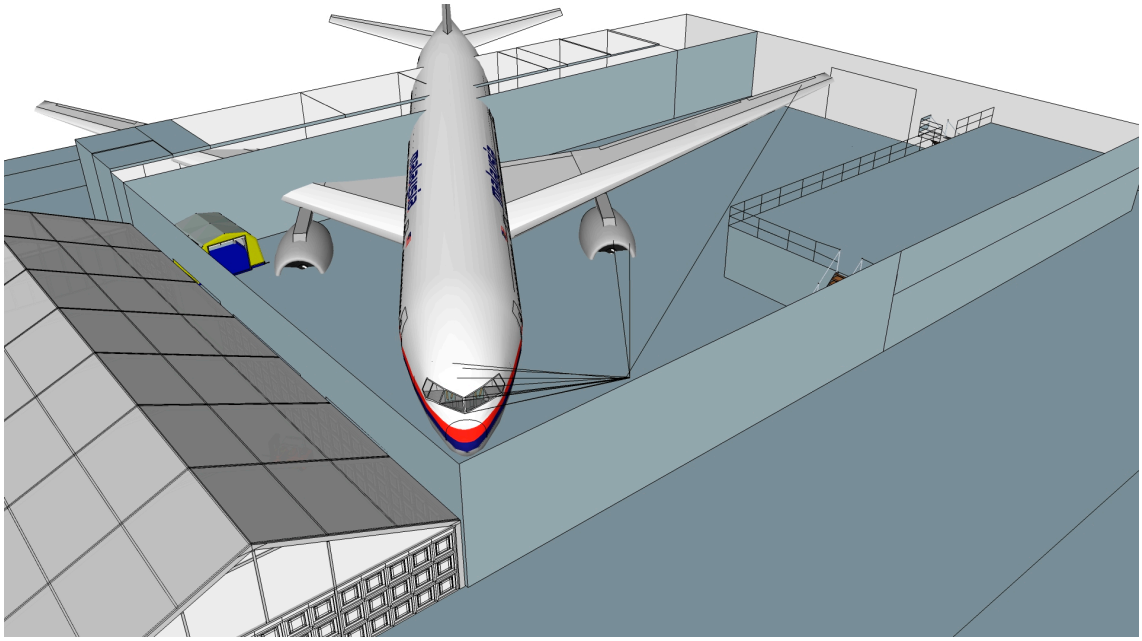

Figure 31: Overview of damage origin (not to scale) (Source: DSB)

2.12 Fragments found

In the wreckage of the cockpit several non-aircraft fragments were found that are assessed to be the high-energy objects, or parts of the high-energy objects, which penetrated the aircraft from the outside. A number of these fragments have a distinct butterfly or bowtie shape, as the one seen in Figure 32.

.

Figure 32: Bowtie fragment found in the wreckage of the cockpit, size in mm (Source: DSB)

2.13 Damage examination conclusion

Based upon the damage examination on the wreckage of flight MH17 the following conclusions can be drawn:

- The impact damage indicates that the aircraft was hit by small objects originating from outside the aircraft and impacting the structure at high velocity.
- Over 350 hits are present on the wreckage of the cockpit and over 800 hits are estimated in total, accounting for the structure of the cockpit that was not available.
- The origin, density, location, boundary and direction of the damage indicate that the objects originated from a general location outside the aircraft to the left of, and above, the cockpit.
- The damage on the left engine cowling ring and the left wingtip indicates that these parts were hit by objects with a general direction from the front to the rear.
- The pitting observed on the wreckage of the cockpit indicates an explosion in the proximity of the cockpit.
- The size of the penetration damage indicates that the objects that caused the damage to the cockpit had a size in the range of 6-14 mm.
- The size of the penetration damage indicates that the objects that caused the damage to the engine cowling ring had a size in the range of 1-200 mm.
- The regularity of hits on the cockpit indicates that the damage is caused by a preformed fragmentation warhead.
- The fragments found in the wreckage of the cockpit indicate that one type of warhead fragment had a distinctive bowtie shape.

Based on the above points it is concluded that the impact damage on the wreckage of flight MH17 is caused by a warhead with various types of preformed fragments in the 6-14 mm size range, including one type with a bowtie shape, detonating to the left of, and above, the cockpit.

3 Possible scenarios

3.1 Focus of investigation

To investigate the possible cause of the high-energy object damage three scenarios were analysed. These scenarios are based on the following:

1. The high-energy object damage on flight MH17 is caused by the effects of a weapon system from outside the aircraft.
2. Only weapon systems that are operated in the region are taken into account.

3.2 Proliferation

To generate a list of operational weapon systems in the region, a 400 km circle around the last recorded position of the Flight Data Recorder (FDR) has been drawn (Figure 33). Since the maximum range of all known operational missile systems is less than 400 km, this ensures that a missile system would have to be located within this circle at the time of launch. Two countries are located within this circle: Ukraine and Russia. Since no information is available on the exact location of the weapon systems of these two countries within their territories at the time of the crash, all operational weapon systems of both countries are taken into account. There is no evidence to suggest that weapon systems from countries other than Ukraine and Russia were present in the region.

Figure 33 Circle with a 400 km radius around the last recorded position of the FDR (Source: Google earth)

3.3 Specific scenarios

Based on the criteria mentioned above, initially three scenarios using specific weapon systems were derived. These scenarios and corresponding weapon systems were selected based on their operational characteristics. Later on in the investigation the number of investigated weapon systems was expanded to be able to exclude complete classes of weapon systems.

4 Scenario 1: Air-to-Air Gun

4.1 Su-25 (Frogfoot)

The specific Air-to-Air Gun scenario focuses on the Sukhoi Su-25, NATO designation: Frogfoot (Figure 34). The Su-25 is a single-seat, twin-engine, subsonic, low altitude, ground attack aircraft. It was designed from the outset as a dedicated Close Air Support (CAS) attack aircraft to provide support for ground troops that are in close contact with enemy forces. Its main task is to engage enemy ground forces, including tanks and armoured vehicles. Its role is comparable to that of the American Fairchild Republic A-10 Thunderbolt.

Figure 34: Su-25

4.2 Su-25 Performance

The performance of the Su-25 is optimized for low altitude and will be mediocre at best at higher altitudes. Its ceiling is limited but the aircraft is assessed to be able to reach 33,000 feet (10,058 meter), the altitude flight MH17 was flying at. The published service ceiling of 7,000 meter (around 23,000 feet) is for physiological reasons because the aircraft is not equipped with a pressurized cockpit. Oxygen is available for the pilot through the oxygen mask to allow operation at altitudes above 10,000 feet (around 3,000 meter) and the pilot is assessed to be able to briefly operate the aircraft at 33,000 feet.

The two jet engines of the Su-25 do not have afterburner capability, which limits available power. Therefore the climb to 33,000 feet is assessed to take relatively long (around 5 minutes) compared to less than 2 minutes for an afterburner equipped aircraft. The manoeuvrability at 33,000 feet is assessed to be very limited.

The maximum attainable True Airspeed (TAS) of the Su-25 at 33,000 feet was calculated. As can be seen in Table 1 this airspeed falls well short of the airspeed flight MH17 was flying at. This rules out a pursuit profile where the attacking aircraft approaches the target aircraft from behind.

Table 1: Airspeed comparison

	Speed TAS [knots]	Speed TAS [km/h]
MH17	484 (actual)	896 (actual)
Su-25	405 (maximum)	750 (maximum)
Speed difference	79	146

4.3 Air-to-Air Guns overview

The investigation was expanded to cover all air-to-air gun capable aircraft in the region. Table 2 and Table 3 give an overview of the combat aircraft armed with guns, including the Su-25 Frogfoot, operated by the Russian Federation and Ukraine. Each aircraft type listed in these tables has one or more versions. The versions of the listed aircraft types either share the indicated gun or do not have an operational gun system; therefore the individual versions are not listed. The Air Force of the former Soviet Union has prohibited the Su-24 from using its gun as a result of two crashes where premature ammunition detonation was a factor. Since 1983, the Su-24 flies with a functional gun but without gun ammunition. It is expected that the Ukrainian Air Force has also prohibited the use of the gun on the Su-24. In the remainder of this text, the words gun and cannon will be used interchangeably.

Table 2: Ukrainian combat aircraft and their guns

Gun type Aircraft type	GSh-30	GSh-301	GSh-6-23	Rounds of ammunition
Sukhoi Su-24			✓	0
Sukhoi Su-25	✓			250
Sukhoi Su-27		✓		150
Mikoyan MiG-29		✓		150

Table 3: Russian Federation combat aircraft and their guns

Gun type Aircraft type	GSh-30	GSh-301	GSh-6-23	Rounds of ammunition
Sukhoi Su-24			✓	0
Sukhoi Su-25	✓			250
Sukhoi Su-27		✓		150
Sukhoi Su-30		✓		150
Sukhoi Su-33		✓		150
Sukhoi Su-34		✓		150
Sukhoi Su-35		✓		150
Mikoyan MiG-29		✓		150
Mikoyan MiG-31			✓	260

4.4 Gsh-30

The GSh-30 is a twin-barrel automatic aircraft cannon (Figure 35). The calibre of this cannon is 30 mm which means that the actual projectiles (bullets) leaving the barrel have a diameter of 30 mm.

Figure 35: GSh-30 aircraft cannon (Source: airforce.ru)

4.5 Gsh-301

The GSh-301 is a single-barrel automatic aircraft cannon (Figure 36). The calibre of this cannon is 30 mm.

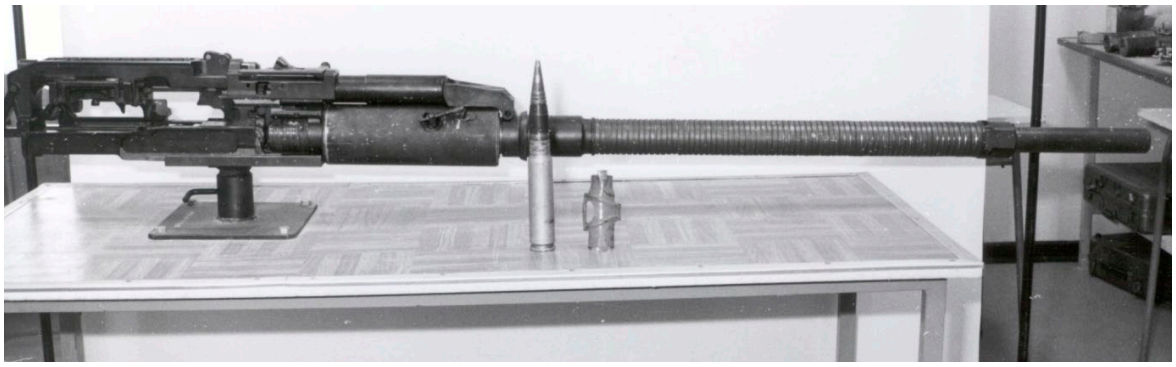

Figure 36: GSh-301 cannon

4.6 Gsh-6-23

The GSh-6-23 is a six-barrel, rotating automatic aircraft cannon (Figure 37). The calibre of this cannon is 23 mm.

Figure 37: GSh-6-23 (Source: afwing.com)

4.7 Attack geometry

The high-energy object hits that have been identified are located on the left front and upper side of the cockpit and the front of the left engine cowling ring. This eliminates the most common attack direction for a gun attack: from the rear. In order for an attacking aircraft to have hit flight MH17 on the left, front side, a left frontal attack would have to be flown. In this attack profile the closing velocity between the two aircraft is very high, leaving little time for proper aim and firing of the gun. At the end of the attack, the attacking aircraft has to break away to

avoid a mid-air collision. This makes a left frontal attack a very difficult and dangerous manoeuvre.

4.8 Visual identification

Because of the dynamics involved in an air-to-air gun attack, a gun sight is used to visually aim the aircraft and the gun onto the target. The distance at which an effective gun attack can be performed is limited. Within these short ranges, a large aircraft such as the Boeing 777 will be clearly identifiable as a civilian airliner by the attacking pilot. Therefore, an erroneous visual identification is assessed to be highly unlikely.

4.9 Number of rounds

Over 350 high-energy object hits have been identified on the wreckage of the cockpit of flight MH17 and over 800 hits are assessed to have hit the cockpit in total, accounting for the structure that was not available. Table 2 and Table 3 show that the analysed aircraft carry a maximum of 150-260 rounds which means that no aircraft could have produced this number of hits due to a lack of ammunition. Also the number of projectiles (bullets) that will hit an airborne target in a left frontal hemisphere attack is calculated to be several dozen at best; much less than number of hits found on the wreckage of flight MH17.

4.10 Density

The density of the hits on an airborne target is assessed to be no more than around 2 per square meter due to the difficulty in aiming, dispersion of the gun and the dynamics of the attack manoeuvre. This is much less than the maximum density of around 250 hits per square meter found on the wreckage of flight MH17.

4.11 Direction

Gun projectiles will travel in approximately parallel trajectories towards the target. As seen in Section 2.10 the back traced trajectories of the high-energy objects hitting flight MH17 all converge to a general location close to the aircraft and are therefore not parallel.

4.12 Type of damage

A 23-mm or 30-mm armour-piercing projectile leaves a hole in a thin-walled metal structure, such as that of an airliner, with a more or less round or elliptical shape, with ragged edges, which are bent inwards. The size of the hole is at least equal to, but generally more than the calibre of the projectile. Measurement of the high-energy object damage on a wreckage panel of flight MH17 showed that

the average size of the holes in the panel is around 11 mm. A 23-mm or 30-mm armour piercing projectile is not able to produce an 11 mm hole. An example of the type of impact damage of a 30 mm armour-piercing projectile fired by a GSh-30 cannon can be seen in Figure 38 and Figure 39. A 23-mm or 30-mm high-explosive projectile is designed to penetrate its target and explode after penetration. Hence fragment damage will be generated from the inside, while the blast of the explosion will deform the structure from inside out. If high explosive-incendiary projectiles are used, additional fire damage is to be expected on the inside of the target from the incendiary component of the projectile. The above mentioned types of damage have not been observed on the wreckage of flight MH17.

Figure 38: GSh-30 projectile damage (Source: YouTube)

Figure 39: GSh-30 projectile damage detail (Source: YouTube)

4.13 Air-to-Air Gun scenario conclusion

The damage observed on the wreckage is not consistent with the damage caused by an air-to-air gun in number of hits, density of hits, direction of trajectories and type of damage. The high-energy object damage on the wreckage of flight MH17 is therefore not caused by an air-to-air gun.

5 Scenario 2: Air-to-Air Missile

5.1 R-60

The specific Air-to-Air Missile scenario focuses on the R-60 (NATO designation: AA-8 'Aphid') air-to-air missile (Figure 40). The R-60 is a small, infrared-guided missile for short-range air-to-air engagements. The missile is compatible with most operational Soviet designed combat aircraft. The missile length is 2.10 meter and the missile mass is 44 kg, making it one of the smallest dedicated air-to-air missiles in service.

Figure 40: R-60 air-to-air missile (Source: topwar.ru)

5.2 Attack geometry

The infrared seeker of the R-60 is assessed to have almost no head-on capability against an airliner type target. The seeker needs a clear line of sight to the hot engine parts at the rear of the engine to obtain a solid lock. This means that the only feasible attack geometry is a tail-on attack whereby the attacking aircraft engages the target from the rear hemisphere.

5.3 Visual identification

The R-60 missile is only used for Within Visual Range (WVR) engagements, meaning that it is limited to visual attacks only. The distance at which the seeker of the R-60 can obtain a solid lock on an airliner is limited and at that distance a large aircraft such as the Boeing 777 will be clearly identifiable as a civilian airliner by the attacking pilot.

5.4 Amount of damage

The R-60 is equipped with a small 3 to 3.5 kg warhead with limited effectiveness. The amount of high-energy object damage found on the wreckage of flight MH17 is not consistent with a warhead of this size.

5.5 Type of damage

The R-60 is equipped with a rod warhead. In this type of warhead a large number of metal rods are aligned cylindrically on the outside of the explosive material. Figure 41 shows this construction in a burned AIM-7 Sparrow warhead. This particular warhead is around 11 times heavier than the R-60 warhead. Figure 42 shows the damage mechanism of a continuous rod warhead. In a continuous rod warhead the rods are welded together at the ends. The blast expands the rods outward creating an expanding continuous circle of rods. Where this circle hits, the target will receive a continuous cut through the skin and any underlying structure. Figure 43 shows an example of the damage caused by the continuous rod warhead of the aforementioned AIM-7 Sparrow missile. In a discrete rod warhead the rods are separate and not welded together. Figure 44 shows an example of the damage caused by discrete rods on an aircraft structure. Both types of rod warhead damage were not observed on the wreckage of flight MH17.

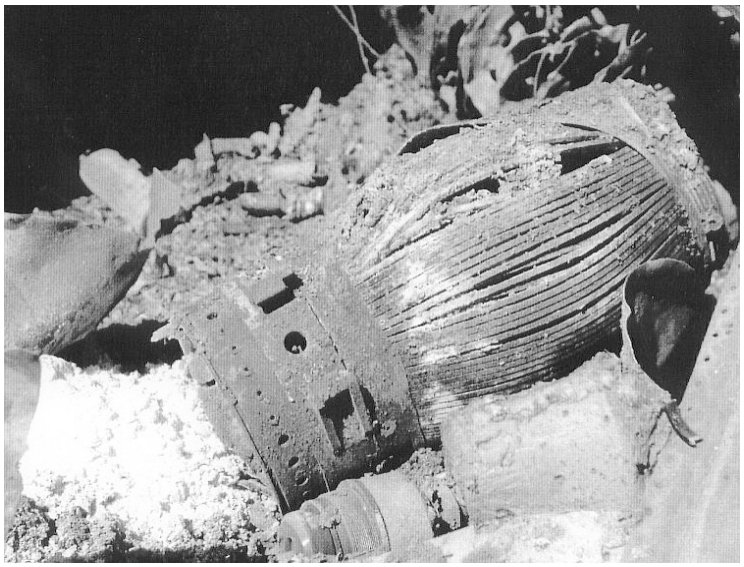

Figure 41: Burned AIM-7 Sparrow rod warhead (Source: zianet.com)

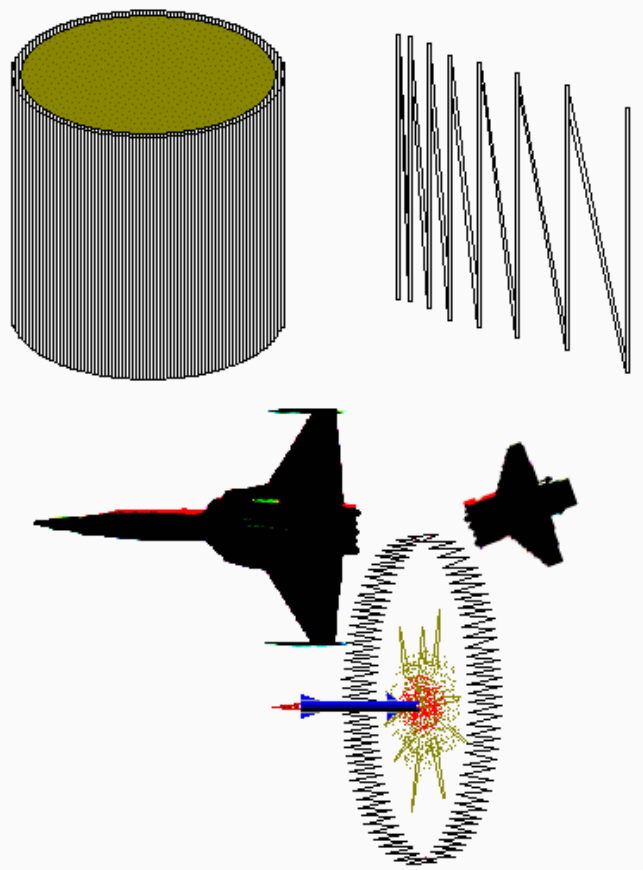

Figure 42: Continuous rod warhead damage mechanism (Source: Wikipedia)

Figure 43: AIM-7 Sparrow continuous rod warhead damage (Source: navalofficer.com.au)

Figure 44: Discrete rod damage (Source: PPRuNe.org)

5.6 Used materials

The rods of the R-60 are made of depleted uranium. No traces of depleted uranium were found on the wreckage of flight MH17.

5.7 R-60 Air-to-Air Missile scenario conclusion

The damage observed on the wreckage is not consistent with the damage caused by the warhead of the R-60 air-to-air missile in amount of damage, type of damage and used materials. The damage on the wreckage of flight MH17 is therefore not caused by the R-60 air-to-air missile.

5.8 Air-to-Air Missile overview

Table 4 and Table 5 give an overview of the air-to-air missiles operated by the Russian Federation and Ukraine. Each missile type listed in these tables has one or more versions. The versions of the listed missile types share the indicated warhead; therefore the individual versions are not listed.

Table 4: Ukrainian air-to-air missiles

Missile	Warhead type	Warhead weight [kg]
R-27	Rod	39
R-60	Rod	3 - 3.5
R-73	Rod	8

Table 5: Russian Federation air-to-air missiles

Missile	Warhead type	Warhead weight [kg]
R-27	Rod	39
R-33	Fragmentation	47
R-37	Fragmentation	60
R-40	Fragmentation	38
R-60	Rod	3 - 3.5
R-73	Rod	8
R-77	Rod	22.5

Since no rod warhead damage was observed on the wreckage of flight MH17 the air-to-air missiles using a rod warhead cannot have caused this damage. Purely based upon warhead type, only the Russian Federation long range missiles R-33, R-37 and R-40 could potentially have caused the damage seen on the wreckage. Because the fragments used in these warheads do not include the distinctive bowtie fragments found in the wreckage, these warheads cannot have caused the damage to the wreckage of flight MH17.

5.9 Air-to-Air Missile scenario conclusion

The damage observed on the wreckage is not consistent with the damage caused by the rod warheads used by most air-to-air missiles. The fragments of the fragmentation warheads used by other air-to-air missiles are not consistent with the bowtie fragments found in the wreckage. The damage on the wreckage of flight MH17 is therefore not caused by an air-to-air missile.

6 Scenario 3: Surface-to-Air Missile

6.1 Surface-to-Air Missile overview

Around 20 types of surface-to-air missiles operational in the Russian Federation and Ukraine that are capable of engaging a target at an altitude of 33,000 feet are identified. All of these missiles use radar guidance and are equipped with a fragmentation warhead. It is assessed that only the 9M38 family of missiles from the BUK family of surface-to-air missile systems are equipped with a fragmentation warhead that uses the unique bowtie shaped fragments found in the wreckage of flight MH17. This information is confirmed by weapon experts of the Russian Federation Investigation Team as well as a representative of Almaz-Antey, the largest Russian weapon manufacturer and manufacturer of the BUK surface-to-air missile system. The Surface-to-Air Missile scenario therefore focuses solely on the 9M38 family of missiles used by the BUK family of surface-to-air missile systems.

6.2 BUK Surface-to-Air Missile system

The Surface-to-Air Missile (SAM) scenario focuses on the 9K37 BUK surface-to-air missile system, NATO designation SA-11/SA-17. The BUK is a medium range, low-to-high altitude, mobile air defence system with semi-active radar guided missiles. The system was designed in the former Soviet Union as a further development of its predecessor, the 2K12 KUB (NATO designation SA-6). The BUK became operational in 1979 and has since then gone through several upgrades. Table 6 shows the different versions of the BUK.

Table 6: Versions of the BUK Surface to Air Missile system

System name	**BUK**	**BUK-M1**	**BUK-M1-2**	**BUK-M2**
System designation	9K37	9K37M1	9K37M1-2	9K40
NATO designation	SA-11	SA-11a	SA-11b	SA-17
TELAR designation	9A310	9A310M1	9A310M1-2	9A317
Missile designation	9M38	9M38 9M38M1	9M38M1 9M317	9M317
Initial Operational Capability (year)	1979	1983	1998	2007

6.3 BUK TELAR

The launching vehicle is called a Transporter Erector Launcher and Radar (TELAR). As can be seen in Table 6, several TELARs are capable of launching two missile types. The three 9A310 family of TELARs are virtually indistinguishable

from each other from the outside. The 9A317 TELAR can be recognized by the smaller radome compared to the 9A310 family of TELARs. The large radome of the 9A310 family of TELARs can be seen on the left side of the rotating upper structure in Figure 45.

Figure 45: BUK-M1-2 Surface-to-Air Missile System Transporter Erector Launcher and Radar (TELAR) 9A310M1-2 with two 9M317 missiles (left) and two 9M38M1 missiles (right)

6.4 Normal operation

In normal operation the BUK surface-to-air missile system operates as a unit of several tracked vehicles consisting of:

- one Target Acquisition Radar (TAR) vehicle
- one Command Post (CP) vehicle
- several Transporter Erector Launcher and Radar (TELAR) vehicles
- several Transporter Erector Launcher and Loader(TELL) vehicles
- technical, maintenance and other support vehicles

A normal mode of operation starts when the Command Post receives target information from higher echelons and uses the Target Acquisition Radar (TAR) to search for and detect possible targets. When a potential target has been detected and identified as hostile, the fire control radar of the TELAR will acquire and track the target. When the target gets within range, it is possible to engage the target with one or more missiles from the TELAR and/or TELL.

6.5 Autonomous operation

Unlike its predecessor, the KUB, each BUK TELAR is equipped with its own fire control radar located inside the radome. This gives the TELAR the possibility to search and engage a target independently and operate completely autonomously, even if an attack has disabled the Target Acquisition Radar and/or the Command Post. The TELAR is limited to mechanically scan a limited sector (whereas the TAR could provide 360° coverage), with an antenna designed to track a target. The time needed for the TELAR to detect a target is longer than during normal operation, but the system is still able to engage a target using only the TELAR without any outside assistance.

6.6 BUK missile

Table 7 gives an overview of the operational versions of the BUK missile in the region and the corresponding warheads.

Table 7: BUK missile versions

Missile designation	**Warhead designation**	**Warhead fragments**
9M38	9N314	filler, square
9M38	9N314M	bowtie, filler, square
9M38M1	9N314M	bowtie, filler, square
9M317	9N318	unknown

As can be seen in this table the 9M38 missile can be equipped with both the 9N314 and the 9N314M warhead. A representative of Almaz-Antey, the manufacturer of the BUK surface-to-air missile system, stated that only the 9N314M warhead contains bowtie fragments. The 9M38 and the 9M38M1 missiles are virtually indistinguishable from each other from the outside. The 9M317 missile has a different, higher span and shorter chord wing design compared to the earlier missiles, as can be seen in Figure 45. In the remainder of the text the designation 9M38(M1) will be used to refer to both the 9M38 and the 9M38M1.

The 9M38(M1) missile is 5.55 m long, weighs 690 kg and uses semi-active radar homing with Proportional-Navigation guidance. In semi-active radar homing systems the active tracking radar on the ground (in the case of the BUK system in the TELAR) illuminates the target with a beam of radar energy. The passive radar seeker in the nose of the missile tracks the radar energy reflected off the target. Proportional-Navigation guidance systems use the target tracking information obtained from the seeker to steer the missile directly towards the predicted collision point with the target. After launch, the missile will perform an initial

course correction towards this collision point. If the target does not manoeuvre or change its velocity, the missile will follow a more or less straight path towards this collision point for the remainder of the flight.

6.7 Altitude capability

Both the BUK fire control radar and the missile have an altitude capability of well over 33,000 feet, the altitude flight MH17 was flying at.

6.8 Proximity fuse

The 9M38(M1) missile is equipped with both an impact and a proximity fuse. The impact fuse detonates the warhead when the missile directly hits the target. In most cases however the missile will not directly hit the target but will pass the target in close proximity. The proximity fuse uses a beam of radar energy in a cone with an angle forward with respect to the missile axis to sense the presence of a target. When a part of the target passes through the beam, the target is detected and after a short delay the fuse will detonate the missile's warhead.

The proximity fuse of the 9M38(M1) missile was simulated during the approach towards the Boeing 777. This showed that, because of the forward looking angle of the proximity fuse, the aircraft is detected before the missile body passes the aircraft. Almaz-Antey, the manufacturer of the BUK surface-to-air missile system, provided additional information on the working and the delay timings of the proximity fuse of the 9M38(M1) missile [4]. Based on this information and the simulations of the missile approach it was assessed that the time required for the proximity fuse to detect the aircraft, execute the required delay and detonate the warhead to the left of, and above, the cockpit, falls within the limits of normal operation. The location of the damage on the wreckage of flight MH17 is therefore consistent with the effects of a warhead detonation point outside the aircraft initiated by the proximity fuse of the 9M38(M1) missile.

6.9 Amount of damage

The 9M38(M1) missile carries a relatively large 70 kg high-explosive fragmentation warhead. The amount of damage observed on the wreckage of flight MH17 is consistent with a warhead of this size.

6.10 Type of damage

The 9M38(M1) missile has a preformed fragmentation warhead. In a preformed fragmentation warhead the case surrounding the explosive material is composed of one or more layers of preformed (separate) fragments. This is different to the natural fragmentation of a smooth case and the controlled fragmentation of a

grooved or scored case in which cases the fragments are formed by the explosive force at the moment of detonation. The fragments of a preformed fragmentation warhead are arranged regularly around the circumference of the warhead and stay intact after detonation of the warhead. The damage of preformed fragmentation is different from that of natural and controlled fragmentation and very distinct in that the preformed fragments give a regular pattern of fragment impacts on the target. These regular impacts are observed in the cockpit area of the wreckage. The type of damage observed on the wreckage of the cockpit of flight MH17 is consistent with the type of damage caused by the preformed fragmentation warhead of the 9M38(M1) missile.

6.11 Bowtie fragments

In the wreckage of flight MH17 several non-aircraft related, foreign fragments were found that are assessed to be the high-energy objects, or parts of the high-energy objects, that penetrated the aircraft from the outside. A number of these fragments found in the cockpit area have a distinct butterfly or bowtie shape, as the one seen in Figure 46. These fragments are recognized as one of the three types of preformed fragments used in the 9N314M warhead of the 9M38 and 9M38M1 missiles. Figure 47 shows these bowtie fragments in an inert 9N314M warhead. Accounting for deformation and abrasion due to explosion and impact, the bowtie fragments found in the wreckage of flight MH17 match the 9N314M warhead bowtie preformed fragments in shape, size and weight.

Figure 46: Bowtie fragment found in the wreckage of the cockpit, size in mm (Source: DSB)

Figure 47: 9N314M warhead fragments in an inert warhead (Source: photo.quip.ru)

6.12 Number and density of hits

The 9N314M warhead is composed of approximately 7800 preformed fragments of three different shapes which are arranged in two layers. See Figure 48 and Figure 49 for pictures of a 9N314M warhead. A digital reconstruction of the 9N314M warhead fragment arrangement can be seen in Figure 50. The inner layer consists of bowtie and filler fragments and spans the entire length of the warhead. The outer layer consists of squares and spans approximately three quarters of the warhead length as can be seen by the change in diameter on the top half of Figure 49. The number and density of hits on the wreckage of the cockpit is consistent with the number and density of hits expected from the detonation of a 9N314M warhead.

Figure 48: 9N314M warhead fragment layers in an inert warhead. (Source: photo.quip.ru)

Figure 49: 9N314M warhead (Source: Almaz-Antey)

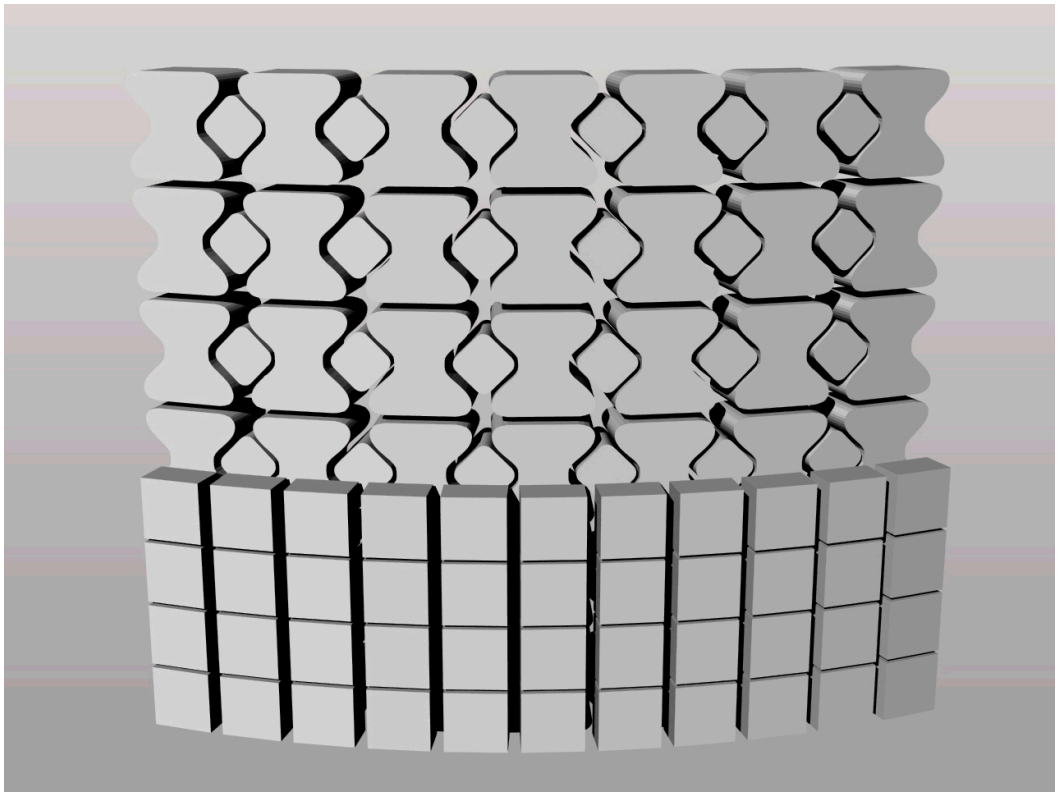

Figure 50: Digital reconstruction of BUK warhead fragment arrangement (Source: AAIB)

6.13 Fragment dimensions

In Section 2.6 the size of the penetration damage was found to range from 6 mm to 14 mm. Figure 51 shows the fragment dimensions of bowtie, filler and square fragments of the 9N314M warhead. Comparison shows that the fragment dimensions of the 9N314M warhead matches with the damage size found on the cockpit area of the wreckage.

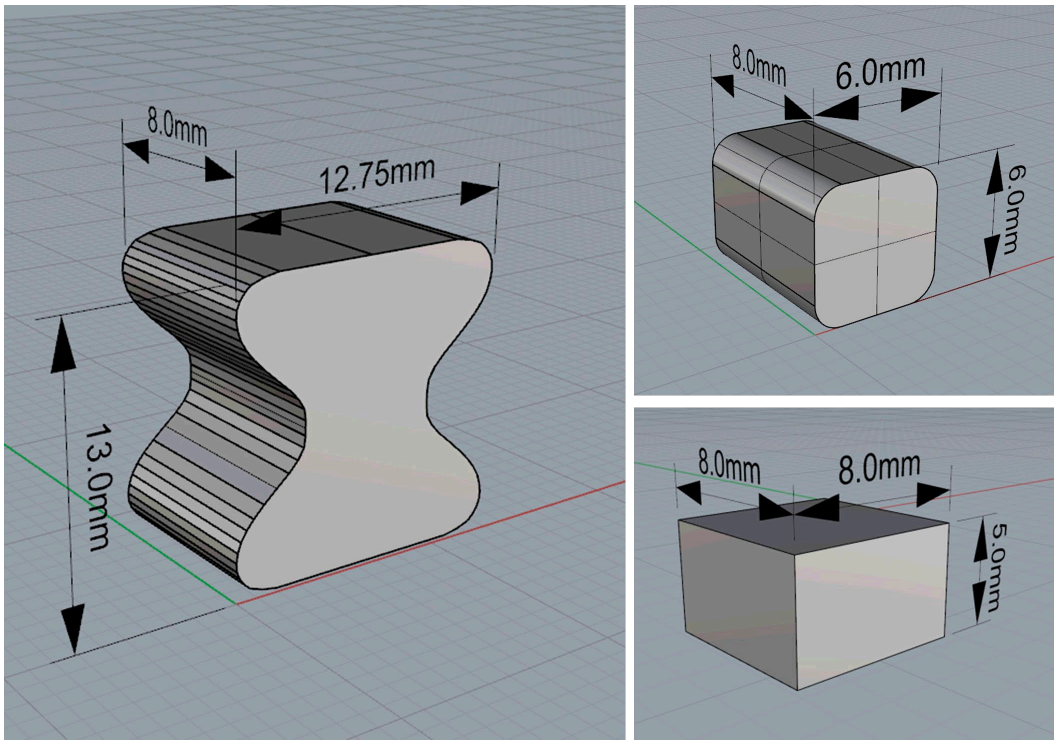

Figure 51: Fragment dimensions of bowtie (left), filler (upper right) and square (lower right) (Source: AAIB)

6.14 Static warhead model

In a warhead using preformed fragments, the separate fragments are ejected by the blast and propagate away from the detonation point in an expanding ring-like pattern. Figure 52 shows an example of the fragmentation pattern of a stationary, horizontal high-explosive fragmentation warhead detonation. This fragmentation pattern creates a bounded fragment spray zone as can be seen in Figure 53. The static fragment spray zone boundaries are defined by the angle α_1 with respect to the missile (warhead) axis of the leading (most forward) fragment and the angle α_2 of the trailing (most rearward) fragment. Theoretically, all the fragments that propagate away from the detonation will be within the fragment spray zone between these two boundaries. Using a mathematical model of the 9N314M warhead these angles were calculated by TNO together with the fragments initial velocities V_0 [3].

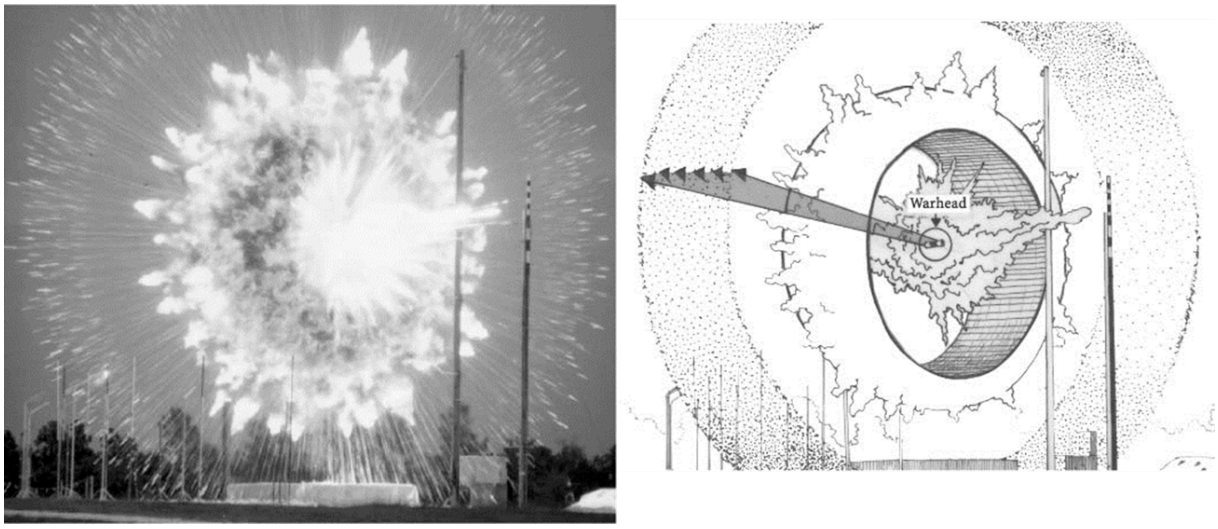

Figure 52: Fragmentation pattern of a stationary, horizontal high-explosive fragmentation warhead detonation. (Source: The Fundamentals of Aircraft Combat Survivability Analysis and Design, Robert E. Ball)

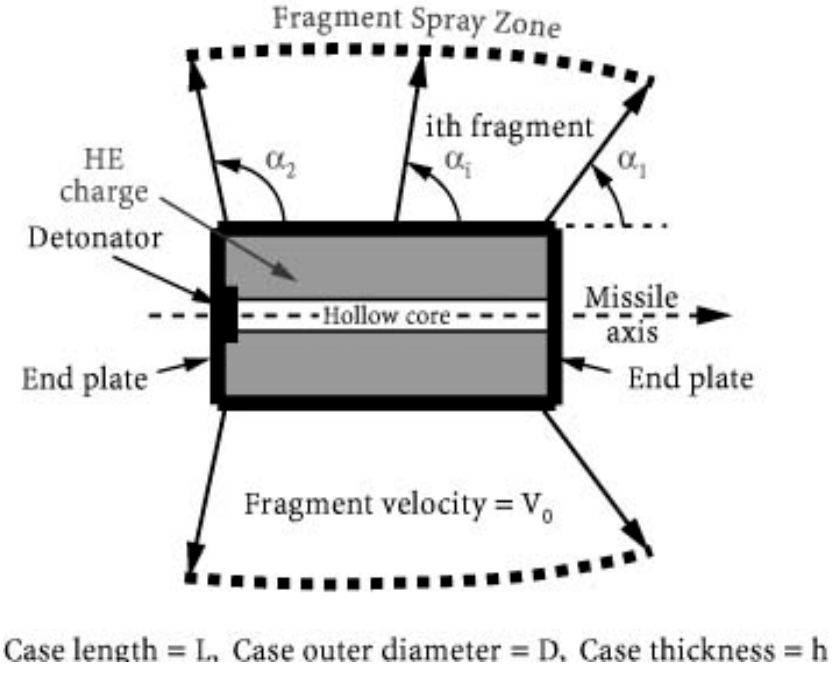

Figure 53: Fragment Spray Zone of a static detonation of a cylindrical warhead. (Source: The Fundamentals of Aircraft Combat Survivability Analysis and Design, Robert E. Ball)

6.15 Dynamic fragmentation pattern

The fragmentation pattern including the fragment spray zone and the initial velocities calculated in the previous section are valid for a stationary detonation only. In an actual engagement the warhead travels with the missile at the same speed as the missile. The forward velocity of the warhead (and missile) needs to be added to the fragment initial velocities in a vector sum. This changes the angles of the fragmentation pattern forward, as can be seen on the right hand side of Figure 54.

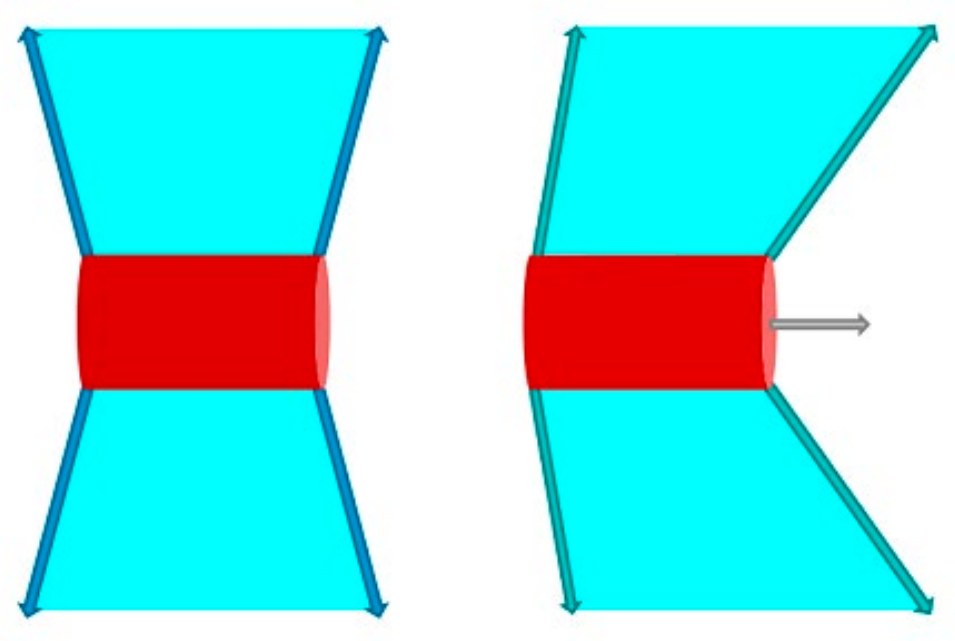

Figure 54: Change in fragmentation pattern from static (left) to dynamic (right) due to warhead forward velocity

6.16 Primary and secondary fragmentation pattern

The fragmentation pattern described in the previous sections is called the primary or main fragmentation pattern. All the preformed fragments (bowtie, filler and square) that will become the high-energy objects are found within the fragment spray zone defined by this primary fragmentation pattern. However the warhead is not located at the very front of the missile. In front of the warhead the guidance, electronics, proximity fuse and seeker sections are located. Upon detonation of the warhead these sections will disintegrate and create a secondary fragmentation pattern moving forward in the direction of flight of the missile in a cone as shown in green in Figure 55.

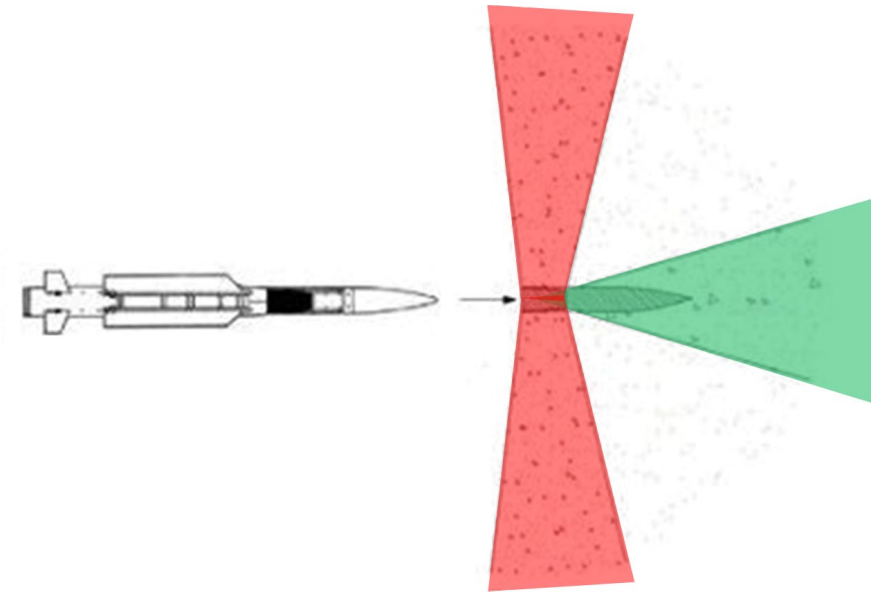

Figure 55: Primary (red) and secondary (green) fragmentation pattern. (Source: verkkomedia.org)

6.17 Matching modelled and observed fragmentation damage

Using the dynamic primary fragmentation pattern calculated in the previous sections, the known speed of flight MH17 and a 3D-model of the Boeing 777, a simulation model of the location, the impact angles and the boundaries of the primary fragmentation on the fuselage of the Boeing 777 was constructed. Light was used to visualize the area of the fuselage exposed to the dynamic primary fragment spray of the warhead. This Fragmentation Visualization Model was used to match the calculated fragment spray of the warhead with the observed high-energy object damage on the cockpit as described in Chapter 2 in both location, boundary and impact angle.

The best match was obtained for a detonation location of the warhead of 0.25 metres ahead of the aircraft's nose, 3 metres to the left of, and 3.7 metres above the tip of the nose. The missile was travelling at a speed of approximately 700 m/s in the opposite direction to the direction of flight of the aircraft, approaching 7 degrees from below and 20 degrees from the right with respect to the aircraft forward axis.

Using the warhead detonation point with this location, speed and orientation (angles), the Fragmentation Visualization Model matches the damage observed on the wreckage of flight MH17. Examples are:

- The boundary and angle of the grazing high-energy object impacts on the roof of the cockpit (Figure 56).
- The boundary and angle of the grazing high-energy object impacts on the left-hand side of the cockpit (Figure 57).
- The boundary of the high-energy object impacts on the captain's (left-hand) front cockpit window and the area of highest damage density around the middle cockpit window on the left-hand side (Figure 58).
- The unaffected area of the cockpit on the right-hand side (Figure 59).

The boundary and angles of the damage on the wreckage of the cockpit of flight MH17 is consistent with the primary fragmentation pattern of the 9N314M warhead.

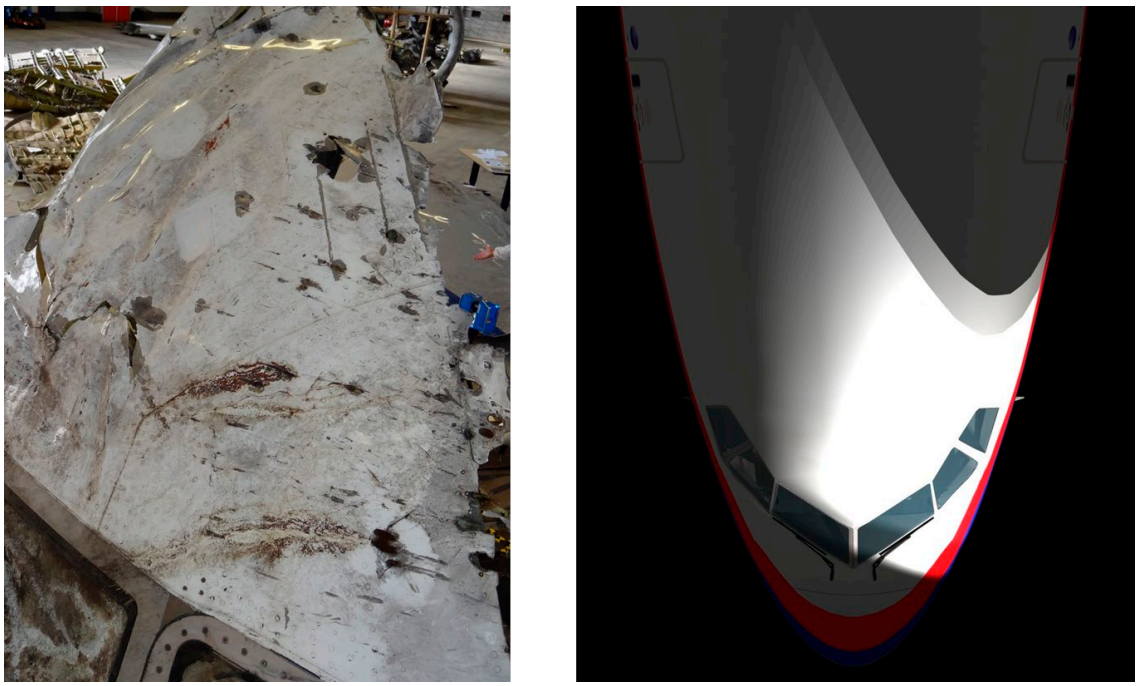

Figure 56: Matching of high-energy object impacts on cockpit roof

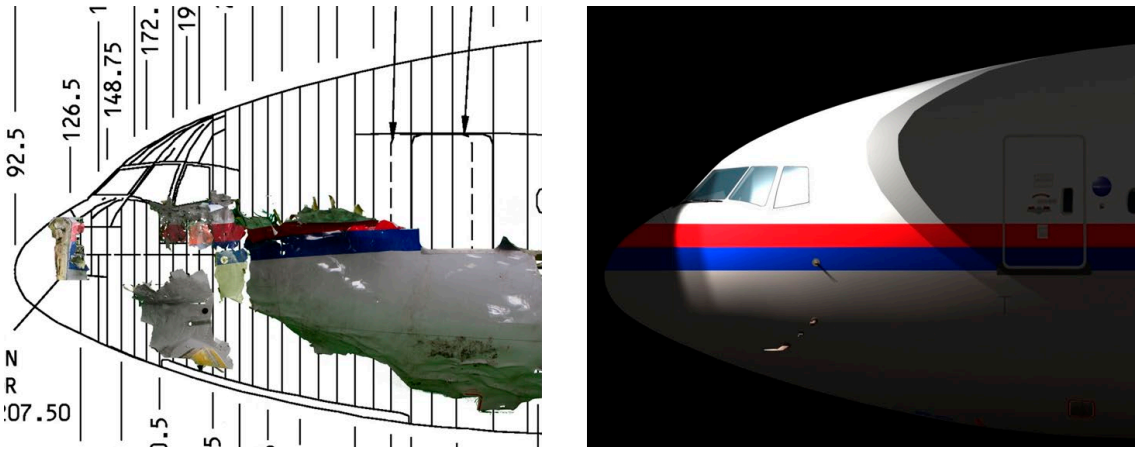

Figure 57: Matching of high-energy object impacts on cockpit left-hand side

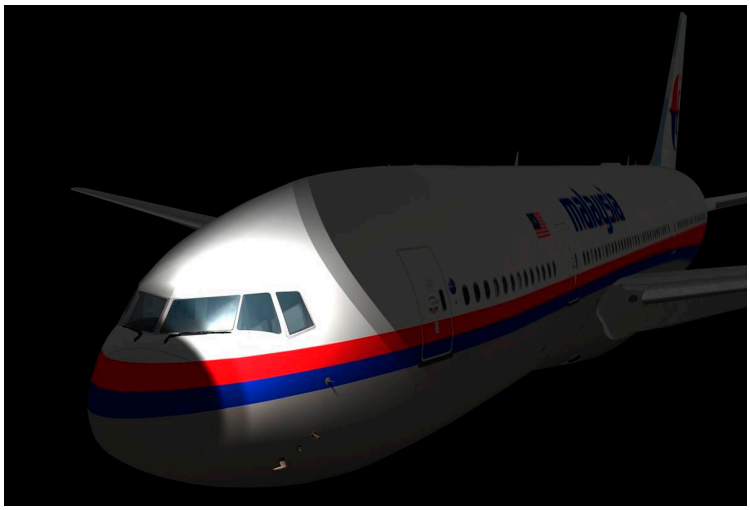

Figure 58: Perspective view of Fragmentation Visualization Model match

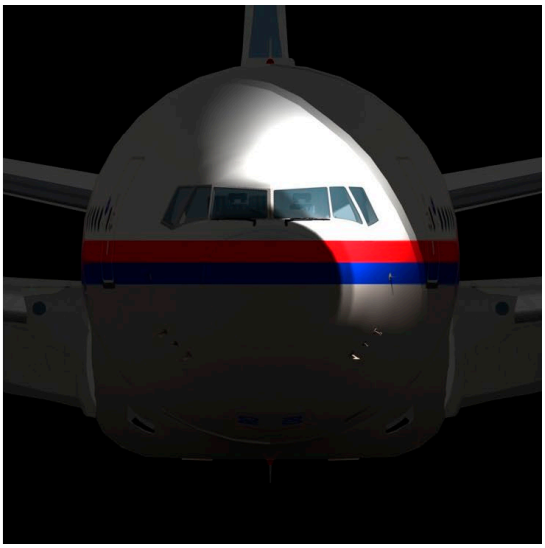

Figure 59: Matching of high-energy object impacts, front view

6.18 Kinematic Fragment Spray Pattern Simulation

Using the fragment initial velocities and aerodynamic calculations, the deceleration due to aerodynamic drag of the various fragments was modelled and calculated. The results of these calculations were used to perform a kinematic simulation of the fragment spray pattern. This simulation includes missile speed, speed of the Boeing 777, initial fragment speeds and fragment deceleration and was used to validate the results obtained from the Fragmentation Visualization Model. The location, orientation and airspeed of the warhead at the time of detonation of the Fragmentation Visualization Model could be validated with this Kinematic Fragment Spray Pattern Simulation.

To visualize these results slow-motion movies of the simulation were made. Figure 60 shows several frames of this simulation in a top down view. The red cylinder represents the boundary of the fastest fragments and the yellow cylinder the boundary of the slowest. The fragment spray pattern cloud is a complex shape located in between these two cylinders.

On detonation the missile disintegrates and forms the secondary fragmentation described in Section 6.16. Extrapolating the missile trajectory in the Kinematic Fragment Spray Pattern Simulation shows that the secondary fragmentation caused by this disintegration, as depicted in Figure 55, will travel in the direction of the left engine. This secondary fragmentation damage is consistent with the damage observed on the left engine cowling ring shown in Section 2.11. The secondary damage on the left wingtip is assessed to be caused by a larger missile fragment grazing the upper surface of the wingtip.

Figure 61 shows several frames of the movie with a perspective view from the left-hand side. The location and the boundaries where the fragments impact the fuselage match with the observed damage as seen in Section 2.9.

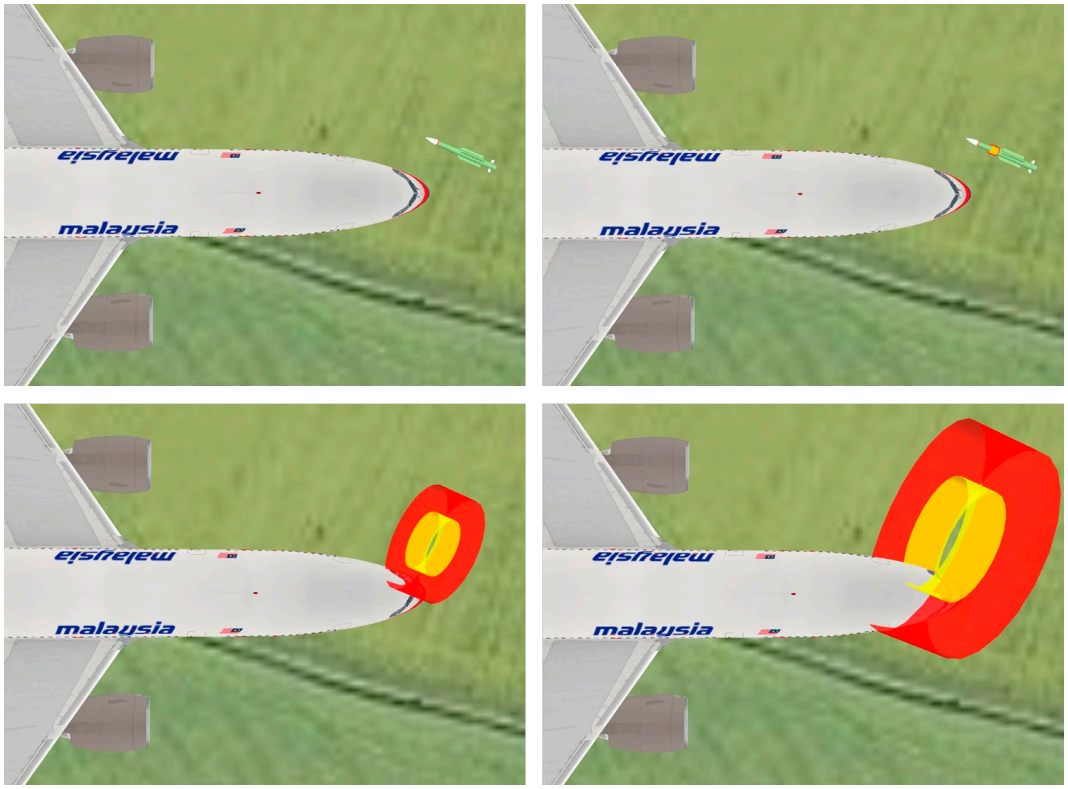

Figure 60: Kinematic Fragment Spray Pattern Simulation showing boundary of fastest (red) and slowest (yellow) fragments, top down view

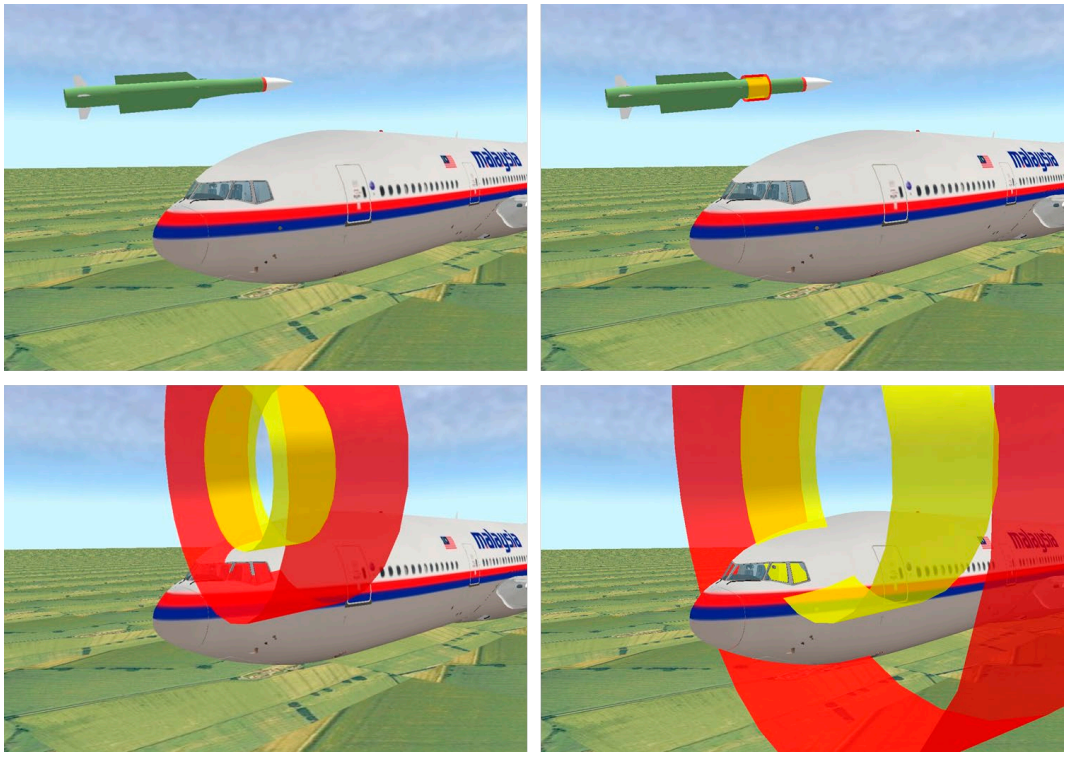

Figure 61: Kinematic Fragment Spray Pattern Simulation showing boundary of fastest (red) and slowest (yellow) fragments, perspective view

6.19 Missile flyout simulation

The advanced six degrees of freedom missile flyout simulation WEST (Weapon Engagement Simulation Tool) was used to assess that the missile end speed and orientation (angles), obtained from the damage matching of the previous sections, could be realized by an engagement of flight MH17 by the 9M38(M1) missile. This simulation is based on a validated aerodynamic missile flyout model, a rocket engine thrust profile model and models of the radar seeker, missile guidance logic and autopilot, and is able to accurately calculate the missile trajectory and kinematic performance. Figure 62 shows two frames of this missile flyout simulation.

Figure 62: Missile flyout simulation

6.20 Missile Launch Area

The area from where the missile was launched was calculated using the damage matching study described in the previous sections, and the last recorded Flight Data Recorder position of flight MH17. The damage matching study determined the weapon's end conditions (orientation and airspeed at detonation) associated with the best match of the damage observed on the wreckage. Using the missile simulation software WEST, numerous missile launches were simulated over a grid of launch locations on the ground. At each launch location, the missile launch angles in the horizontal and vertical plane were varied to minimize the difference between the simulated end conditions and those associated with the best match of the damage.

To account for a number of uncertainties in weapon performance and guidance, a range of orientation angles and airspeeds around the best match end conditions was defined. The launch locations for which the simulated end conditions are within this defined range constitute the possible launch area. This means that a missile launched from within this area can result in the damage

pattern observed on the wreckage. This launch area is determined by missile kinematic performance, aerodynamics, seeker limits and is independent of the launching platform. Figure 63 shows this calculated missile launch area on the map together with the flown track and last known FDR position of flight MH17.

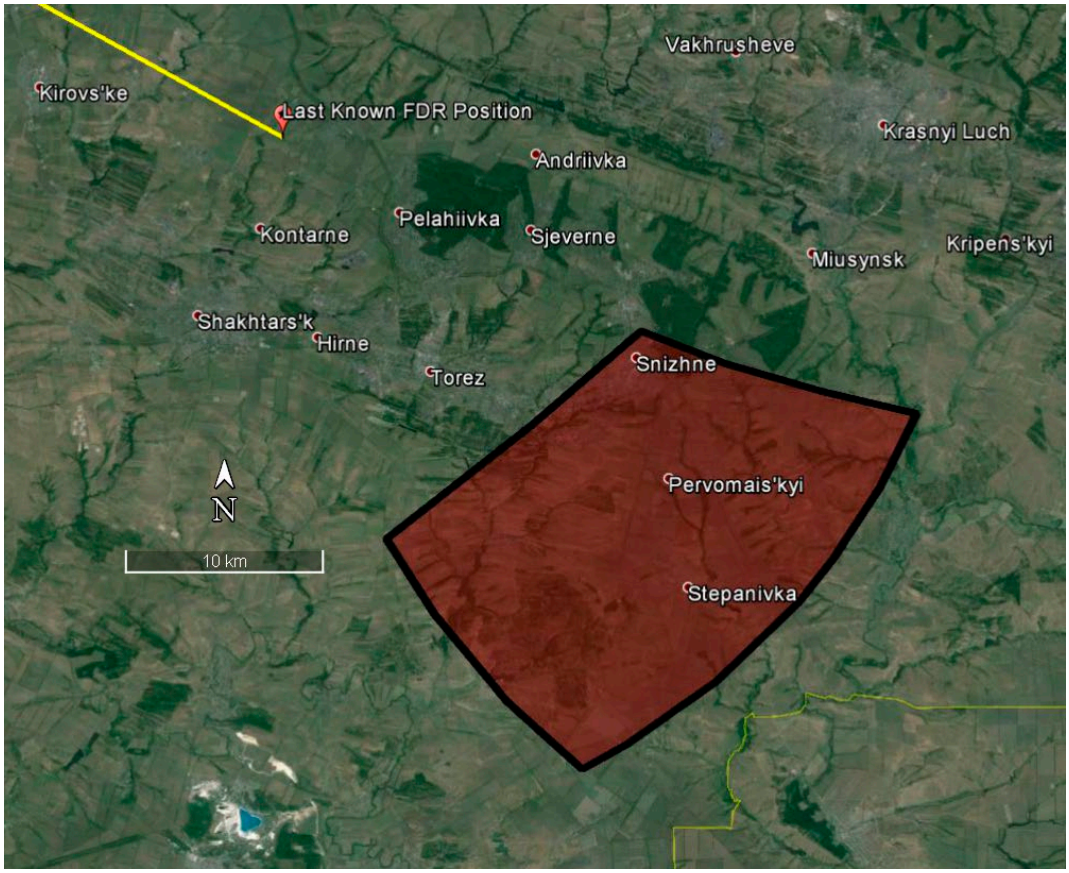

Figure 63: Calculated Missile Launch Area (Source: Google earth, CNES/Astrium, US Dept of State Geographer, DigitalGlobe)

6.21 Surface-to-Air Missile scenario conclusion

Based upon the observed damage on the wreckage of flight MH17 and the capabilities of the BUK surface-to-air missile system, the following conclusions can be drawn:

- The BUK missile system is capable of engaging a Boeing 777 with the airspeed and at the altitude flight MH17 was flying at.
- The location of the damage on the wreckage is consistent with the effects of a warhead detonation point initiated by the proximity fuse of the 9M38(M1) missile.
- The amount of damage on the wreckage is consistent with a relatively large warhead such as the 70 kg 9N314M BUK warhead.
- The type of damage on the wreckage of the cockpit is consistent with the type of damage caused by the primary fragmentation of the 9N314M preformed fragmentation warhead.
- The boundary and impact angles of the damage on the wreckage of the cockpit are consistent with the primary fragment spray pattern of the 9N314M warhead detonating to the left of, and above, the cockpit.
- The number and density of hits on the wreckage of the cockpit is consistent with the number and density of hits expected from the detonation of the 9N314M warhead.
- The size of the penetration damage on the wreckage of the cockpit is consistent with the size of the fragments of the 9N314M warhead.
- The damage on the left engine cowling ring and the left wingtip is consistent with the secondary fragmentation pattern of the 9M38(M1) missile.
- The bowtie fragments found in the wreckage of the cockpit are consistent with the bowtie fragments unique to the 9N314M warhead.
- The direction of both the primary and the secondary damage on the wreckage is consistent with the missile orientation and end speed as obtained by a 9M38(M1) BUK missile launched from a launch area in the east of Ukraine.

Based on these points it is concluded that the damage observed on the wreckage of flight MH17 is caused by the 9N314M warhead of the 9M38(M1) BUK surface-to-air missile launched from a launch area in the east of Ukraine.

7 Summary of findings

The impact damage due to high-energy objects on the wreckage of flight MH17 was investigated. This investigation led to the following conclusions:

Damage examination

- The impact damage indicates that the aircraft was hit by small objects originating from outside the aircraft and impacting the structure at high velocity.
- Over 350 hits are present on the wreckage of the cockpit and over 800 hits are estimated in total, accounting for the structure of the cockpit that was not available.
- The origin, density, location, boundary and direction of the damage indicate that the objects originated from a general location outside the aircraft to the left of, and above, the cockpit.
- The damage on the left engine cowling ring and the left wingtip indicates that these parts were hit by objects with a general direction from the front to the rear.
- The pitting observed on the wreckage of the cockpit indicates an explosion in the proximity of the cockpit.
- The size of the penetration damage indicates that the objects that caused the damage to the cockpit had a size in the range of 6-14 mm.
- The size of the penetration damage indicates that the objects that caused the damage to the engine cowling ring had a size in the range of 1-200 mm.
- The regularity of hits on the cockpit indicates that the damage is caused by a preformed fragmentation warhead.
- The fragments found in the wreckage of the cockpit indicate that one type of warhead fragment had a distinctive bowtie shape.

Based on the above points it is concluded that the impact damage on the wreckage of flight MH17 is caused by a warhead with various types of preformed fragments in the 6-14 mm size range, including one type with a bowtie shape, detonating to the left of, and above, the cockpit.

Air-to-Air Gun scenario

The damage observed on the wreckage is not consistent with the damage caused by an air-to-air gun in number of hits, density of hits, direction of trajectories and type of damage. The high-energy object damage on the wreckage of flight MH17 is therefore not caused by an air-to-air gun.

Air-to-Air Missile scenario

The damage observed on the wreckage is not consistent with the damage caused by the warhead of the R-60 air-to-air missile in amount of damage, type of damage and used materials. The damage observed on the wreckage is not consistent with the damage caused by the rod warheads used by most air-to-air missiles. The fragments of the fragmentation warheads used by other air-to-air missiles are not consistent with the bowtie fragments found in the wreckage. The damage on the wreckage of flight MH17 is therefore not caused by an air-to-air missile.

Surface-to-Air Missile scenario

Based upon the observed damage on the wreckage of flight MH17 and the capabilities of the BUK surface-to-air missile system, the following conclusions can be drawn:

- The BUK missile system is capable of engaging a Boeing 777 with the airspeed and at the altitude flight MH17 was flying at.
- The location of the damage on the wreckage is consistent with the effects of a warhead detonation point initiated by the proximity fuse of the 9M38(M1) missile.
- The amount of damage on the wreckage is consistent with a relatively large warhead such as the 70 kg 9N314M BUK warhead.
- The type of damage on the wreckage of the cockpit is consistent with the type of damage caused by the primary fragmentation of the 9N314M preformed fragmentation warhead.
- The boundary and impact angles of the damage on the wreckage of the cockpit are consistent with the primary fragment spray pattern of the 9N314M warhead detonating to the left of, and above, the cockpit.
- The number and density of hits on the wreckage of the cockpit is consistent with the number and density of hits expected from the detonation of the 9N314M warhead.
- The size of the penetration damage on the wreckage of the cockpit is consistent with the size of the fragments of the 9N314M warhead.
- The damage on the left engine cowling ring and the left wingtip is consistent with the secondary fragmentation pattern of the 9M38(M1) missile.
- The bowtie fragments found in the wreckage of the cockpit are consistent with the bowtie fragments unique to the 9N314M warhead.
- The direction of both the primary and the secondary damage on the wreckage is consistent with the missile orientation and end speed as obtained by a 9M38(M1) BUK missile launched from a launch area in the east of Ukraine.

Based on these points it is concluded that the damage observed on the wreckage of flight MH17 is caused by the 9N314M warhead of the 9M38(M1) BUK surface-to-air missile launched from a launch area in the east of Ukraine.

8 References

1. Robert E. Ball, *The Fundamentals of Aircraft Combat Survivability Analysis and Design*, Second Edition, American Institute of Aeronautics and Astronautics, 2003.

2. Dutch Safety Board, *Preliminary report Crash involving Malaysia Airlines Boeing 777-200 flight MH17*, The Hague, September 2014.

3. TNO, TNO 2015 M11094, *Damage reconstruction due to impact of high-energetic particles on Malaysia Airlines flight MH17*, Rijswijk, August 2015.

4. Almaz-Antey, Materials on the characteristics of the BUK missiles requested by the NLR experts, Moskou, 29 July 2015.

WHAT IS NLR?

The NLR is a Dutch organisation that identifies, develops and applies high-tech knowledge in the aerospace sector. The NLR's activities are socially relevant, market-orientated, and conducted not-for-profit. In this, the NLR serves to bolster the government's innovative capabilities, while also promoting the innovative and competitive capacities of its partner companies.

The NLR, renowned for its leading expertise, professional approach and independent consultancy, is staffed by client-orientated personnel who are not only highly skilled and educated, but also continuously strive to develop and improve their competencies. The NLR moreover possesses an impressive array of high quality research facilities.

***NLR** – Dedicated to innovation in aerospace*

www.nlr.nl